JBC Papers in Press. Published on January 25, 2006 as Manuscript M511598200
The latest version is at http://www.jbc.org/cgi/doi/10.1074/jbc.M511598200

Effects of Coumarate 3-Hydroxylase Down-regulation on Lignin Structure

John Ralph,*[1,2] Takuya Akiyama,[1] Hoon Kim,[1,3] Fachuang Lu,[1,2] Paul F. Schatz,[1] Jane M. Marita,[1] and Sally A. Ralph.[4]

From the [1]U.S. Dairy Forage Research Center, USDA-Agricultural Research Service, Madison Wisconsin 53706, USA; [2]Department of Forestry, and [3]Department of Horticulture, University of Wisconsin, Madison, Wisconsin 53706, USA; [4]U.S. Forest Products Laboratory, USDA-Forest Service, Madison, Wisconsin 53705, USA.

M. S. Srinivasa Reddy,[5] Fang Chen,[5] and Richard A. Dixon.[5]

From the [5]Plant Biology Division, Samuel Roberts Noble Foundation, Ardmore, Oklahoma 73401, USA.

Down-regulation of the gene encoding 4-coumarate 3-hydroxylase (C3H) in alfalfa massively but predictably increased the proportion of *p*-hydroxyphenyl (P) units relative to the normally dominant guaiacyl (G) and syringyl (S) units. Stem levels of up to ~65% P (from wild-type (WT) levels of ~1%) resulting from downregulation of C3H were measured by traditional degradative analyses as well as 2D ^{13}C–^{1}H correlative NMR methods. Such levels put these transgenics well beyond the P:G:S compositional bounds of normal plants; *p*-hydroxyphenyl levels are reported to reach a maximum of 30% in gymnosperm severe compression wood zones but are limited to a few percent in dicots. NMR also revealed structural differences in the interunit linkage distribution that characterizes a lignin polymer. Lower levels of key β-aryl ether units were relatively augmented by higher levels of phenylcoumarans and resinols. The C3H-deficient alfalfa lignins were devoid of β–1-coupling products, highlighting the significant differences in the reaction course for *p*-coumaryl alcohol *vs* the two normally dominant monolignols, coniferyl and sinapyl alcohols. A larger range of dibenzodioxocin structures was evident, in conjunction with an approximate doubling of their proportion. The nature of each of the structural units was revealed by long-range ^{13}C–^{1}H correlation experiments. For example, although β-ethers resulted from coupling of all three monolignols with the growing polymer, phenylcoumarans were formed almost solely from coupling reactions involving *p*-coumaryl alcohol; they resulted from both coniferyl and sinapyl alcohol in the WT plants. Such structural differences form a basis for explaining differences in digestibility and pulping performance of C3H-deficient plants.

The effects on lignin structure of perturbing one crucial step in the monolignol biosynthetic pathway remain to be addressed. Genes encoding all of the enzymes in Fig. 1 have been identified, and the effects of perturbing (by down- and/or up-regulation in transgenic plants, or via their knockouts in mutants) all but the C3H/hydroxycinnamoyl transferase (HCT) steps have been studied in some detail, as reviewed (1-3). Downregulation of some genes, particularly those early in the pathway, may limit the overall flux of metabolites into lignin. In other cases, the distribution of units resulting from the primary monomers (the three monlignols *p*-coumaryl **1a**, coniferyl **1b**, and sinapyl **1c** alcohols, differing in their degree of methoxylation, Fig. 1) may be dramatically altered, sometimes far beyond the limits that have been observed in nature. In some intriguing cases, lignification appears to be able to accommodate phenolics (e.g. 5-hydroxyconiferyl alcohol) that are not normally considered to be lignin monomers when the biosynthesis of the normal monolignols is thwarted (1, 3, 4). Such studies are not only providing rich insights into the lignification process, but are also opening up opportunities for improving the utilization of plant cell walls in a range of natural and industrial processes, e.g. ruminant digestion (5-13) and chemical pulping (2, 14-22).

Fig. 1. Partial monolignol biosynthetic pathway (1). *p*-Coumarate 3-hydroxylase (C3H) is now understood to operate on *p*-coumarate esters of shikimic acid (shown), quinic acid, or possibly others, themselves produced by recently discovered *p*-hydroxycinnamoyl-CoA: quinate shikimate *p*-hydroxycinnamoyltransferases (HCTs) (42). Enzymes on the remainder of the pathway have their standard abbreviations (1): CAD, cinnamyl alcohol dehydrogenase; CCoAOMT, caffeoyl-CoA *O*-methyltransferase; CCR, cinnamoyl-CoA reductase; COMT, caffeic acid *O*-methyltransferase; F5H, ferulate 5-hydroxylase.

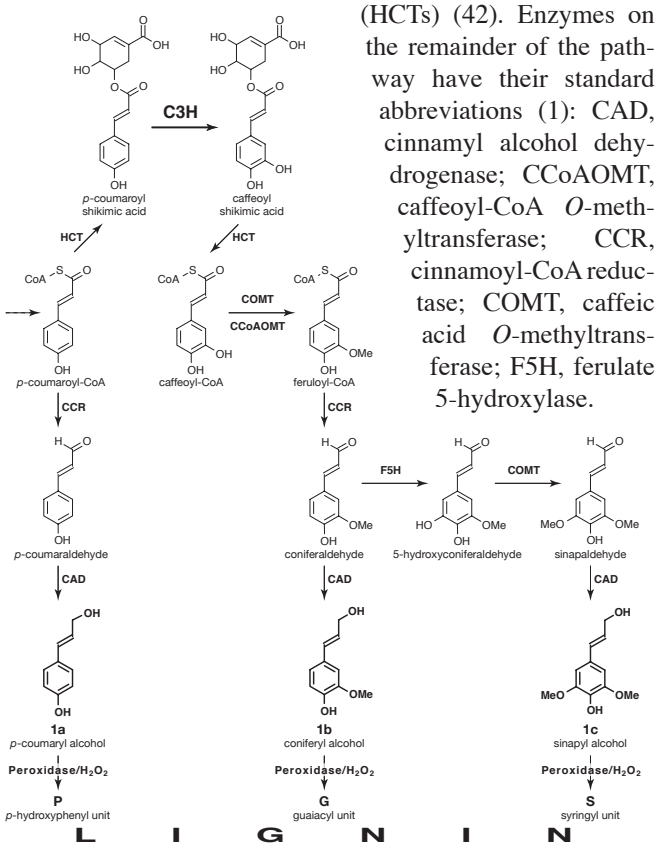

Aromatic hydroxylation steps are considered key reactions in plant secondary metabolism, in part due to their irreversibility. Ferulate 5-hydroxylase (F5H), now often called coniferaldehyde 5-hydroxylase (CAld-5H) to more accurately reflect the preferred substrate (23, 24), is the crucial enzyme allowing syringyl lignin production via the monolignol sinapyl alcohol **1c**. An Arabidopsis mutant deficient in F5H has no syringyl lignin component (25, 26). Like gymnosperms, it produces guaiacyl-rich lignins, derived almost exclusively from the monolignol coniferyl alcohol **1b**. Up-regulation of F5H, as might be anticipated, produces plants with lignins having higher syringyl contents and relatively depleted in guaiacyl units (G). Analyses of lignins suggest syringyl (S) contents of up to about 92% in F5H-upregulated Arabidopsis (25), and as high as 93% in poplar or aspen (27, 28). Such syringyl levels are comparable to the highest reported in nature (29), with kenaf bast fiber lignin being among the highest at 85-94% (30, 31). In poplar and aspen, the following methylation step via caffeic acid 3-*O*-methyl transferase (COMT), also operating at the aldehyde level and therefore misnamed (32), appears to be able to accommodate the increased flux from coniferaldehyde to 5-hydroxyconiferaldehyde to produce sinapaldehyde and ultimately sinapyl alcohol **1c** (27). In Arabidopsis, however, evidence suggests that the COMT is not able to keep pace with the increased 5-hydroxyconiferaldehyde production, since the lignins have a significant component derived from 5-hydroxyconiferyl alcohol (33). Novel 5-hydroxyguaiacyl (5HG) benzodioxane structures, which result from incorporation of 5-hydroxyconiferyl alcohol into the lignification scheme, analogously to their normal monolignol counterparts, were the same as those noted in COMT-deficient plants (33-36). The 92% syringyl levels in Arabidopsis therefore derive only from S/(G+S); there is no reliable method to measure 5-hydroxyguaiacyl (5HG) levels, nor to measure S/(G+5HG+S) ratios which truly reflect the monomer distribution.

F5H affects the partitioning between the two major traditional monolignols, coniferyl **1b** and sinapyl **1c** alcohols, Fig. 1. Since plants with no syringyl components (i.e. softwoods) are well known, and natural plants can have a very high syringyl component, perturbing F5H might not be expected to greatly interfere with the requirements of the lignin polymer in the plant. The same is presumably *not* true for C3H, however. Although it is likely that perturbing C3H only affects the monolignol distribution, the monolignol *p*-coumaryl alcohol **1a** does not normally contribute to high levels of *p*-hydroxyphenyl (P) units in normal lignins. Rather, these are minor components, typically just 1-3% (29), in the lignins of both gymnosperms and angiosperms. *p*-Hydroxyphenyl units have long been thought to be significantly higher in grasses (37). They may be, but much of the data has come from incorrectly interpreting the products of degradative methods as deriving from *p*-hydroxyphenyl units in lignin whereas substantial proportions may derive from *p*-coumarate ester moieties adorning the lignins of grasses (37); such *p*-coumarate moieties are not involved in the backbone of the polymer and should not be confused with lignin monomers (38). Softwood compression wood fractions have the richest *p*-hydroxyphenyl unit content, reportedly ranging as high as 30% (39). Nevertheless, even this is below the levels that might be expected via C3H-downregulation.

Chapple's group reported on analyses of a C3H-deficient Arabidopsis *ref8* mutant (40). Degradative methods released *p*-hydroxyphenyl units, but no detectable guaiacyl or syringyl components (41). This is consistent with the key role of the hydroxylase on the pathway toward coniferyl and sinapyl alcohols. C3H in Arabidopsis is now understood to operate on *p*-coumarate esters of shikimic acid (Fig. 1) or quinic acid (not shown), themselves produced by hydroxycinnamoyl transferases (42). The difficulty in securing sufficient cell wall material from these stunted *ref8* mutants has limited more detailed structural studies of the resultant lignins. Yet such studies are required since little is known about the coupling and cross-coupling propensities of *p*-coumaryl alcohol **1a** (in lignification reactions) and therefore little can be predicted about the structure and properties of the lignins that might be expected. More recently, one of our groups has successfully generated transgenic plants of the forage legume alfalfa (*Medicago sativa*) in which C3H levels have been reduced to as low as 5% of the wild-type level (Table 1), in the absence of seriously impaired growth phenotypes (13). A detailed structural analysis of the unusual lignins in these plants is described here.

TABLE 1
Basic Data on Wild-Type (WT) Control and C3H-deficient (C3H-4a, C3H-9a) Alfalfa

	WT	**C3H-9a**	**C3H-4a**
%C3H activity of WT	100	20	5
Days to Early Bud	39	41	48
Days to Bloom	50	51	60-70
Whole Plant			
AcBr Lignin (%ABSL)	9.72	7.38	6.76
Thioacidolysis yield (µm/g)	149	65	54
%P (thio)	2.5	28	55
%G (thio)	66	48	30
%S (thio)	31	24	15
Stems			
%P (DFRC)	3	-	59
%G (DFRC)	51	-	22
%S (DFRC)	46	-	20
EL (enzyme-digested CW)			
%CW after digestion	23.6	-	14.7
%carbohydrates	20.0	-	14.1
%lignin*	80.0		85.9
% soluble (**Ac-EL**) for NMR	38	-	31
ML (dioxane/water milled lignin)			
%carbohydrates	5.1		4.8
%lignin*	94.9		95.2
ML % of CW	1.43	-	1.36
ML % of total Lignin	7.6	-	10.8
AL (acidolysis lignin)			
AL % of CW	2.8	-	0.8
AL % of total Lignin	14.6	-	6.6

Fractions are defined in the Materials and Methods Section; ML = dioxane:water-soluble milled lignin, AL = acidolysis lignin (from the ML residue), EL = enzyme-digested cell wall; Ac- indicates acetylated samples.
*Lignin calculated as 100% - %carbohydrates
ABSL = acetyl bromide-soluble lignin
P = *p*-hydroxyphenyl, G = guaiacyl, S = syringyl, CW = cell wall
thio = thioacidolysis-derived monomers; DFRC = monomers derived from the Derivatization Followed by Reductive Cleavage (method).

MATERIALS AND METHODS

General

All chemicals were purchased from Aldrich (Milwaukee, WI, USA) unless otherwise noted. UV spectra were recorded on DU-800 Series spectrophotometers (Beckman Coulter, Inc., Fullerton, CA) at wavelengths between 400 to 700 nm.

Cell Wall Analytical Methods

Acetyl bromide soluble lignin (ABSL). ABSL lignins were determined using essentially the methods previously described (43), but on a smaller scale (2-5 mg of cell wall). However, neither the WT nor the transgenic alfalfa walls were fully soluble in AcBr. Also, no molar extinction coefficient has been reported for *p*-hydroxyphenyl-rich lignins; a value of 17.2 (as determined for WT alfalfa) was used.

Analytical thioacidolysis. Analytical thioacidolysis to release diagnostic lignin monomers was carried out as described (44). The products were examined by GC-MS. GC (Thermoquest Trace GC 2000) conditions were as follows: DB1 column (25 m x 0.2 mm, 33 μm film thickness, J & W Scientific); initial column temperature, 200 °C, held for 1 min, first ramped at rate of 4 °C/min to 248 °C, ramped at rate of 30 °C/min to 300 °C, held for 25 min; inlet temperature 250 °C. MS (Thermoquest GCQ/Polaris MS) conditions were as follows; ion source temperature, 220 °C, transfer line temperature, 300 °C.

Derivatization Followed by Reductive Cleavage (the DFRC method). DFRC release and quantification of acetylated monolignols by reductive cleavage of β-aryl ethers was performed as described (45, 46).

Neutral sugars and total carbohydrate levels. Neutral sugar residues (glucose, xylose, arabinose, mannose, galactose, rhamnose, and fucose) were quantified by gas chromatography as alditol acetate derivatives (47). Approximate lignin levels in isolated ML and AL fractions were determined simply as 100% minus %carbohydrates.

NMR Spectroscopy

The NMR spectra presented here were acquired on a Bruker Biospin (Rheinstetten, Germany) DMX-750 instrument fitted with a sensitive cryogenically-cooled 5-mm TXI $^{1}H/^{13}C/^{15}N$ gradient probe with inverse geometry (proton coils closest to the sample). Lignin preparations (30-60 mg) were dissolved in 0.5 ml $CDCl_3$; the central chloroform solvent peak was used as internal reference (δ_C 77.0, δ_H 7.26 ppm). We used the standard Bruker implementations of the traditional suite of 1D and 2D (gradient-selected, ^{1}H-detected, e.g. COSY, TOCSY, HSQC, HSQC-TOCSY, HMBC) NMR experiments for structural elucidation and assignment authentication. The fully authenticated NMR data for model compounds will be deposited in the "NMR Database of lignin and cell wall model compounds" available via the internet at http://ars.usda.gov/Services/docs.htm?docid=10491 (48). TOCSY experiments used a 100 ms mixing time; HMBC spectra used an 80 or 100 ms long-range coupling delay. Normal HSQC experiments at 750 MHz typically had the following parameters: acquired from 8.6-2.4 ppm in F_2 (^{1}H) using 1864 datapoints (acquisition time 200 ms), 160-40 ppm in F_1 (^{13}C) using 512 increments (F_1 "acquisition time" 11.3 ms) of 16 or 32 scans with a 1 s inter-scan delay, total acquisition time of 2 h 48 min, or 5 h 34 min; the d_{24} delay was set to 1.72 ms (~1/4J). The higher-resolution inset in Fig. 3b acquired just the sidechain region from 6.8-2.4 ppm in F_2 (^{1}H) using 1336 datapoints (acquisition time 200 ms), 110-40 ppm in F_1 (^{13}C) using 800 increments (F_1 "acquisition time" 30 ms) of 8 scans with a 1 s inter-scan delay, total acquisition time of 2 h 12 min. Processing used typical matched Gaussian apodization in F_2 and squared sine-bell in F_1. HMBC experiments at 750 MHz, Fig. 4, had the following parameters: acquired from 8.6-2.4 ppm in F_2 (^{1}H) using 3k datapoints (acquisition time 329 ms), 180-40 ppm in F_1 (^{13}C) using 400 increments (F_1 "acquisition time" 7.6 ms) of up to 112 scans with a 1 s inter-scan delay, 100 ms long-range coupling delay, total acquisition time of up to 18 h. Processing to a final matrix of 2k by 1k datapoints used typical matched Gaussian apodization in F_2 (LB -80, GB 0.338) and squared sine-bell in F_1. One level of linear prediction in F_1 (32 coefficients) gave improved F_1 resolution but was not required.

Volume-integration of contours in HSQC plots was accomplished more conveniently and more accurately than in the past by using Bruker's TopSpin 1.3 software. For quantification of P:G:S ratios, only the carbon-2 correlations from guaiacyl units, and the carbon-2/6 correlations from syringyl or *p*-hydroxyphenyl units were used, and the guaiacyl integrals were logically doubled. No correction factors were deemed necessary after noting only slight deviations from 1:1:1 volume integral ratios in a range of model dimers and trimers with mixed P/G/S units. For quantification of the various interunit linkage types, the following well-resolved contours (see Fig. 3) were integrated: **A**α, **B**α, **C**α, **D**α, **S**α, **X1**γ and **X7**β, as well as **B**β, **C**β, **D**β, and **S**β as checks. Integral correction factors were determined by acquiring spectra from a range of mixed-unit trimers and tetramers. Such models have an exact integral molar ratio of units, usually 1:1, making this approach superior to using mixtures of more simple models. The models chosen were from our collection in the NMR database (48) (noted as Lib. #), or from a recent study on oligolignol metabolic profiling (49) denoted by just #: acetylated S–(β–O–4)–G–(β–5)–G, compound #39; phenol-methylated acetylated G–(β–O–4)–S–(β–β)–S–(4–O–β)–G, #33; acetylated G–(β–5)–Glycerol, Lib. #262; and an acetylated mixture of a simple GG/G-dibenzodioxocin **3b** (see below) and the β-ether model veratryl-glycerol-β-guaiacyl ether (Lib. #105, acetate #3). The determined relative response factors were: **A**α 1.00, **B**α 0.71, **C**α 1.06, **D**α 0.87, **S**α not determined, **X1**γ possibly 2.0 (not reliably determined), and **X7**β 0.77. These values were used to correct the volume integrals to provide the semi-quantitative estimates of unit ratios in Table 3, but note that these values can only be used here and should not be considered universal — they are dependent upon the spectrometer and acquisition conditions.

Plant Materials

Transgenic alfalfa (*Medicago sativa* cv Regen SY) plants downregulated in C3H transcripts and corresponding enzyme activity were generated as described elsewhere (13). The C3H-4a and C3H-9a lines mentioned herein had 5% and 20% residual C3H-activity compared to the wild-type (WT) control (Table 1).

Lignin Isolation

Stems (internodes 4-10) were harvested from control (WT) and the most heavily C3H-deficient (C3H-4a) alfalfa lines. Lignins were isolated using methods largely described previously (34). Briefly, alfalfa stems were ground and extensively soxhlet-extracted sequentially with water, methanol, acetone, and chloroform. The isolated cell walls were ball-milled for 2.5 h (in 0.5 h on/0.5 h off cycles to avoid excessive sample heating) using a custom-made ball mill using an offset 1/4 hp Dayton motor running at 1725 rpm with rotating (0.2 Hz) stainless steel vessels (12.2 cm diameter, 11.4 cm high) containing ~3.7 kg 5 mm stainless steel ball bearings; total weight of jar and bearings is ~6.15 kg. The ball milled walls (9.90 and 10.10 g for WT and C3H-4a transgenic) were then digested at 30 °C with crude cellulases (Cellulysin, Calbiochem, San Diego, CA 219446 lot #B29887, 40 mg/g of sample, in pH 5.0 acetate buffer, 3 x 48 h, fresh buffer and enzyme each time) leaving all of the lignin and residual polysaccharides totaling 2.338 g (23.6% of the original cell wall, WT) and 1.487 g (14.7%, C3H-4a) (Table 1). Soluble lignins were difficult to extract from alfalfa as has been noted previously (36). Extraction of 1.001 g (WT) and 1.003 g (C3H-4a) with 96:4 dioxane:H_2O, freeze drying, water washing, and filtration of the product using a 10 kDa membrane ultra-filter (YM10-43 mm; Amicon-Millipore Corp., Bedford, MA) to remove water-soluble components (mainly low molecular weight sugars) gave the soluble lignin (ML) fraction (64 mg and 98 mg) containing 5.1% and 4.8% polysaccharides; after correction, this represents approximately 1.43% and 1.36% of the cell wall and 7.6% and 10.8% of the total lignin (Table 1). This ML was acetylated overnight, and water/EDTA washed to remove trace metal contaminants (38, 50), giving the Ac-ML used for NMR. To obtain a further fraction, the residue from the ML extraction was subjected to mild acidolysis (51), to yield fractions AL (see supplementary material) comprising another ~14.6% and 6.6% of the original lignin. Finally, in order to characterize as much of the lignin fraction as possible, the entire polysaccharidase-digested cell wall fraction was subjected to solubilization in DMSO/N-methylimidazole — a solvent shown to dissolve the whole cell wall fraction of ball-milled woods and other plants (52). Dissolution of these alfalfa samples was however incomplete. The polysaccharidase-digested cell walls, 330 and 370 mg from WT and transgenic C3H-4a respectively, yielded 360 and 440 mg of acetylated sample. Chloroform-fractionation yielded 200 and 220 mg soluble fractions, 100 and 130 mg insoluble residue, but 60 and 80 mg in losses. The soluble fraction in chloroform was then subjected to molecular weight fractionation on Biobeads S-X2 (Bio-Rad, Hercules, CA) yielding 137 mg high-MW fractions in each case; a further 29 mg (WT) and 44 mg (C3H-4a) of lower MW material was also recovered but not examined. The fraction of the polysaccharidase-digested cell wall examined by NMR was therefore 38% (WT) and 31% (C3H-4a).

Model Compounds and Polymers

Synthesis of p-coumaryl alcohol dimeric, trimeric and oligomeric coupling and cross-coupling products. The synthesis and characterization of model dimers and oligomers from *in vitro* radical coupling reactions will be described more fully elsewhere once compounds have been separated, fully identified, and the data have been rigorously interpreted.

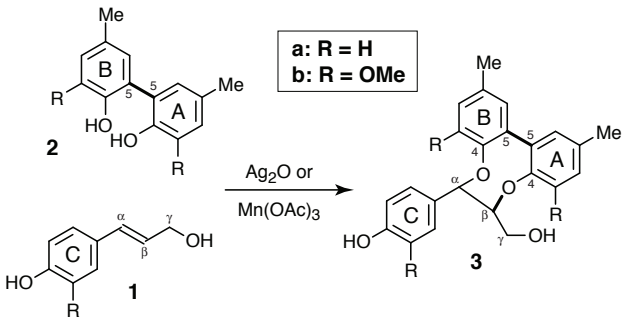

Scheme 1. Preparation of dibenzodioxocin model compounds **3**. In the text, dibenzodioxocin structures are referred to using *p*-hydroxyphenyl (P), guaiacyl (G) and syringyl (S) descriptors for the A, B, and C rings; e.g. the GG/S dibenzodioxocin derives from a sinapyl alcohol (ring C) monomer coupling with a guaiacyl-guaiacyl (GG) 5–5-coupled unit. Bolder bonds (5–5 between rings A and B, β–O–4 between units C and B) are formed during the radical coupling steps.

Synthetic Dehydrogenation Polymers (DHPs). The synthesis of polymers from *p*-coumaryl alcohol alone or copolymers with all three monolignols, used to authenticate the P-aromatic units in alfalfa lignins, are detailed in the Supplementary Material.

Synthesis of a PP/P-dibenzodioxocin Model Compound. A PP/P-type dibenzodioxocin **3a**, 4-(7-hydroxymethyl-2,11-dimethyl-6,7-dihydro-5,8-dioxadibenzo[*a,c*]cyclooctene-6-yl)-phenol, was synthesized in low yield by coupling a simple 5–5-dimer with *p*-coumaryl alcohol using silver (I) oxide (53), Scheme 1. 5,5′-Dimethyl-biphenyl-2,2′-diol **2a** (0.107 g, 0.5 mmol) (54) was dissolved in acetone (5 ml) and silver (I) oxide (0.463 g, 2 mmol) was added. *p*-Coumaryl alcohol **1a** (0.150 g, 1 mmol) (55) in acetone (30 ml) was added slowly to the suspension over 4 h. The mixture was stirred overnight and partially concentrated under reduced pressure at 25 ºC to about 10 ml. The suspension was diluted with EtOAc and washed with saturated NH_4Cl, dried over Na_2SO_4, and the solvent evaporated under reduced pressure. The crude products obtained was submitted to preparative TLC eluting with $CHCl_3$-EtOAc (1:1, v/v) to obtain a fraction containing the dibenzodioxocin. Further separation by preparative TLC (eluent: hexane-EtOAc 2:1, multiple elution) provided compound **3a** (8 mg, 4% yield; attempts will be made to improve this yield in further studies on the dibenzodioxocin components of these samples). NMR ($CDCl_3$): δ_H/δ_C 4.82/86.7 (α), 4.25/86.1 (β), (4.03, 4.12)/63.9 (γ).

Synthesis of a GG/G-dibenzodioxocin Model Compound. The GG/G-type dibenzodioxocin **3b**, 4-(7-hydroxymethyl-4,9-dimethoxy-2,11-dimethyl-6,7-dihydro-5,8-dioxadibenzo[*a,c*]cycloocten-6-yl)-2-methoxy-phenol, was prepared using $Mn(OAc)_3$ in pyridine (56) from 3,3′-dimethoxy-5,5′-dimethyl-biphenyl-2.2′-diol **2b** and coniferyl alcohol **1b**, Scheme 1. Yield 23%. NMR ($CDCl_3$): δ_H/δ_C 4.84/84.5 (α), 4.13/82.8 (β), (4.03, 4.50)/64.1 (γ).

RESULTS

The aim of the current study was to delineate the consequences of C3H down-regulation for lignin structure. More detailed descriptions of the lines analyzed here and other lines with varying C3H levels are reported elsewhere (13). Briefly, plants with less than approximately 15% of wild-type C3H activity (demonstrated using *p*-coumaroyl shikimic acid as the substrate and detecting the production of the caffeoyl shikimic acid, Fig. 1), appeared somewhat smaller at flowering than corresponding vector control lines (see top left picture in Fig. 3). C3H line 4a, with only 5% residual C3H activity, showed delayed flowering by 10-20 days (Table 1). However, C3H line 9a, with approximately 20% residual C3H activity, was of normal size and exhibited delayed flowering by only 1-2 days. The bright red coloration throughout the WT stem cross-section vascular tissue following staining with Mäule reagent, a stain normally used to detect S units in lignin (57), was reduced in the C3H lines to a dark brown coloration with more limited distribution between the major xylem cells, consistent with an overall reduction in S-lignin content (13). The C3H-4a line, with the lowest C3H level, was logically chosen for this initial study to delineate the most extreme structural effects associated with C3H-down-regulation.

Lignin Levels and Aromatic Unit (P:G:S) Distribution

Total forage samples (leaf plus stem) from internodes 1-5 were harvested from the C3H-4a down-regulated and empty vector control lines at the first bud stage. Lignin content was estimated by the acetyl bromide soluble lignin (ABSL) procedure and by total thioacidolysis yield (Table 1). Thioacidolysis also provided estimates of monomer abundance, expressed as relative %P (derived from *p*-coumaryl alcohol **1a**), %G (from coniferyl alcohol **1b**), and %S (from sinapyl alcohol **1c**). ABSL levels of forage samples were significantly reduced in C3H down-regulated lines. These results were magnified in the corresponding total thioacidolysis yields, and sizeable differences were observed in the thioacidolysis yields of the individual P, G and S monomers. The reasons become clear from the NMR analyses (below) showing that the β-ether content is lower in the C3H-deficient plants. Down-regulation of C3H resulted in a massive increase in the proportion of P units in the lignin, and a significant decrease in the ratio of G to total units.

TABLE 2

NMR-derived *p*-Hydroxyphenyl:Guaiacyl:Syringyl (P:G:S) Data for Stem Lignins from Control and C3H-Deficient Plants

Sample	%P	%G	%S
Control Ac-ML	0.8	58	41
Control Ac-AL	0.7	61	39
Control Ac-EL	0.8	58	41
C3H-4a Ac-ML	65	17	18
C3H-4a Ac-AL	68	17	15
C3H-4a Ac-EL	66	16	18

Fractions are defined in the Materials and Methods Section; ML = dioxane:water-soluble milled lignin, AL = acidolysis lignin (from the ML residue), EL = enzyme-digested cell wall; Ac- indicates acetylated samples.
Control is the Wild-type
C3H-deficient transgenic, C3H-4a, has 5% residual C3H levels.

The stem fractions were used for lignin isolation and NMR analysis; some compositional data are given in Table 1. As an independent measure of the wild-type and the C3H-deficient (C3H-4a) lines, the DFRC method gave similar P:G:S ratios as determined for the whole plant by thioacidolysis, Table 1. Both thioacidolysis (44) and the DFRC method (45) release quantifiable monomers from units linked by β-ether bonds. As such, the measured P:G:S ratio is a reflection of the units involved only in so-called uncondensed units. A measure of the actual P:G:S ratio in soluble lignin fractions was also made by NMR (see below, and Table 2). Although the methodology here has not been firmly established, similarly high P-levels were indicated by 2D NMR volume integration.

NMR — Aromatic Region

Changes in the P:G:S distribution in the lignins are most readily visualized from the aromatic region of NMR spectra, particularly the 2D ^{13}C–^{1}H correlation (HSQC) spectra correlating protons with their attached carbons. Figure 2 shows the impressive differences in the aromatic nature of the polymers

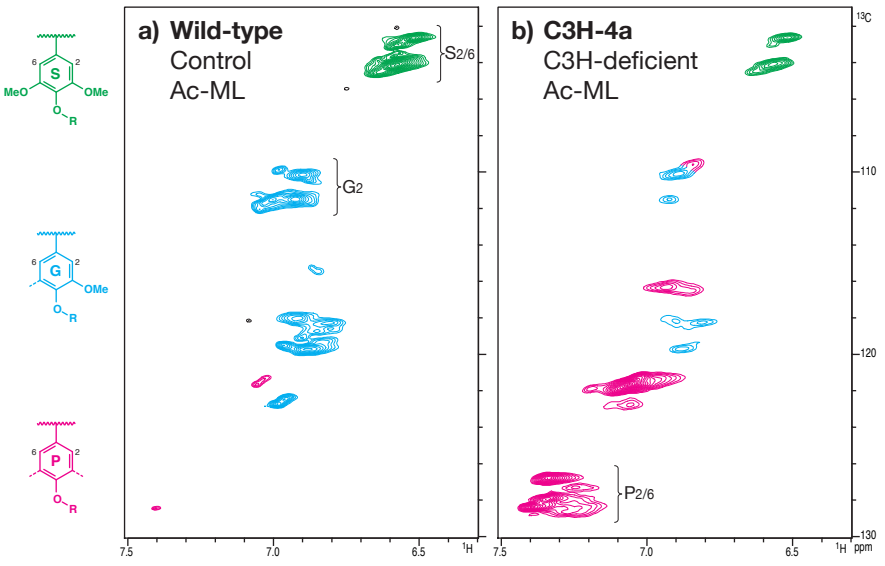

Fig. 2. Partial short-range ^{13}C–^{1}H (HSQC) correlation spectra (aromatic regions only) of milled lignins (ML) isolated from a) the wild-type control and b) the most highly C3H-deficient line, C3H-4a. Traces of *p*-hydroxyphenyl (P) units are seen in the typically syringyl/guaiacyl (S/G) lignin in the wild-type alfalfa, whereas P-units entirely dominate the spectrum in the transgenic. Semi-quantitative volume integrals are given in Table 2. Analogous spectra for the other lignin isolates (acidolysis lignins, AL, and enzyme lignins, EL) are provided in the Supplementary Material.

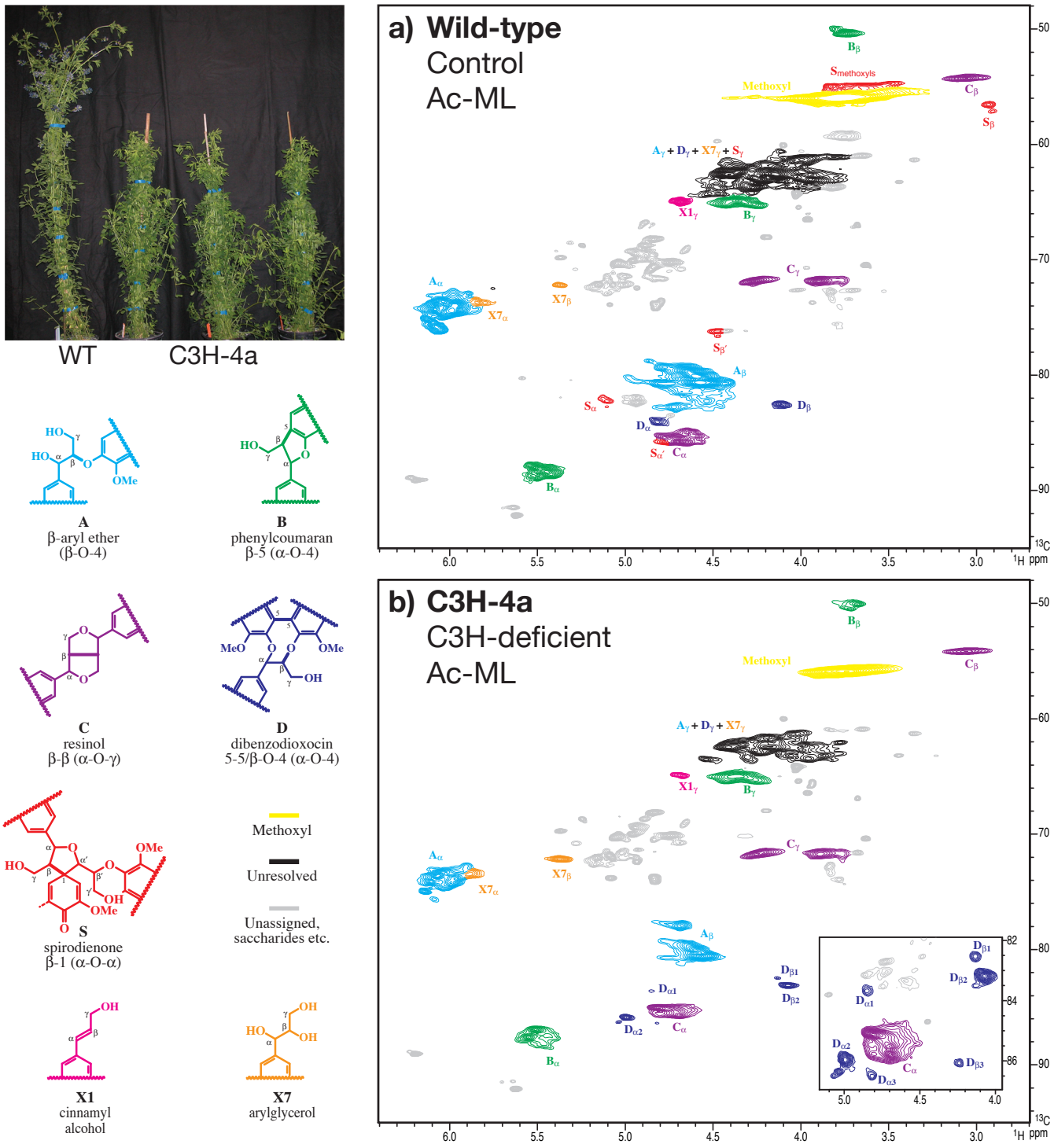

Fig. 3. Partial short-range ^{13}C–^{1}H (HSQC) spectra (sidechain regions) of milled lignins (ML) isolated from a) the wild-type control and b) the most highly C3H-deficient line, C3H-4a. C3H-deficiency, and the incorporation of higher levels of *p*-coumaryl alcohol into the lignin, produces substantial changes in the distribution of interunit linkage types. The absence of spirodienone S units in the transgenic reveals that *p*-coumaryl alcohol does not apparently favor β–1-cross-coupling reactions. Several types of new dibenzodioxocins **D** are more readily seen at the lower contour levels in the more highly resolved partial spectrum in the inset. Note that the contour levels used to display the two spectra were chosen to highlight the structural similarities and differences; with no internally invariant peaks, interpretation of apparent visual quantitative differences needs to be cautious. The upper-left corner photograph shows WT and C3H-4a transgenic plants at the WT flowering stage; pictures of the C3H-9a transgenic and histochemical staining are provided elsewhere (13). Volume integrals and semi-quantitative data are given in Table 3. Analogous spectra for the other lignin isolates (acidolysis lignins, AL, and enzyme lignins, EL) are provided in the Supplementary Material. Interunit type designations **A**-**D**, **S**, **X1** and **X7** follow conventions established previously (1, 3, 58).

TABLE 3
NMR-derived Interunit Linkage Data for Stem Lignins from Control and C3H-Deficient Plants

Sample	%A	%B	%C	%D	%S	%X1	%X7
Control Ac-ML	75	9	9	1.1	0.6	4.8	0.5
Control Ac-AL	80	8	7	0.6	0.2	3.7	0.4
Control Ac-EL	77	8	8	0.7	0.6	4.7	0.6
C3H´ Ac-ML	56	18	16	2.6	-	2.9	4.6
C3H´ Ac-AL	56	16	14	2.1	-	5.3	6.0
C3H´ Ac-EL	53	17	16	1.8	-	5.6	6.6

Fractions are defined in the Materials and Methods Section; ML = dioxane:water-soluble milled lignin, AL = acidolysis lignin (from the ML residue), EL = enzyme-digested cell wall; Ac- indicates acetylated samples.
Control is the Wild-type
C3H-deficient transgenic, C3H-4a, has 5% residual C3H levels.
A = β–O–4 (β-aryl ether); **B** = β–5 (phenylcoumaran); **C** = β–β (resinol); **D** = dibenzodioxocin; **S** = β–1 (spirodienone); **X1** = cinnamyl alcohol endgroup; **X7** = arylglycerol endgroup.

in the wild-type (Fig. 2a) vs the C3H-deficient (C3H-4a line, Fig. 2b) lignins. As established previously (36), alfalfa lignin is a typical, slightly guaiacyl-rich, syringyl-guaiacyl lignin. Syringyl and guaiacyl aromatic resonances are well separated at 750 MHz, but also at lower field. Traces of the *p*-hydroxyphenyl component are visible in this spectrum (Fig. 2a). The lignin from the C3H-deficient alfalfa is strikingly unlike any lignin seen by these investigators. Relatively weak, but diagnostic, syringyl (S) and guaiacyl (G) correlations remain in a spectrum that is overwhelmed by the *p*-hydroxyphenyl (P) correlations. Volume-integration (Table 2) allows reasonable quantification of the differences that are plainly visible. The lignins in all three types of fractions analyzed (the solvent-soluble lignin ML, the acidolysis lignin AL on the residue, and the crude enzyme lignin EL following our cell wall dissolution procedure) all showed similar distributions (see Table 2, and Figures in the Supplementary material). As might be anticipated, the enzyme lignin (EL, the best representative of the whole lignin) has a distribution between that of the easily removed solvent-soluble ML and the most rigorously extracted acidolysis lignin (AL) fraction from the ML residue. This suggests that only minimal partitioning of structure types between the fractions has occurred, and that the isolated solvent-soluble lignin from ball milled material is representative of that from the whole ball-milled cell wall.

NMR — Sidechain Region

The sidechain region only peripherally reflects the changes in the P:G:S distribution, but is rich in detail regarding the types and distribution of interunit bonding patterns present in the lignin fraction.

The control lignin spectrum, Fig. 3a, is typical of a guaiacyl/syringyl lignin containing residual polysaccharides (58). The HSQC spectrum resolves most of the correlations for the various linkage types in the polymer, the exception being in the complex γ-region, where only the correlations from the phenylcoumarans **B** and the cinnamyl alcohol endgroups **X1** are fully resolved. The lignin is seen as being rich in β-aryl ether units **A**, with more modest amounts of phenylcoumaran **B** and resinol **C** units, as is typical for all lignins. Arylglycerol units **X7**, not normally reported, are identified here; it is suspected that they may arise from β-ether units during ball-milling, but can also be produced under oxidative coupling reaction conditions (see Supplementary Material). Their 5-hydroxyguaiacyl analogs have recently been documented in COMT-deficient alfalfa lignins (36). Spirodienone structures **S**, β–1-coupled units only recently authenticated in lignin spectra (59, 60), are readily seen in alfalfa (3). The diagnostic dibenzodioxocins **D** are also relatively newly discovered 8-membered ring structures resulting from radical coupling of a monolignol with a 5–5-coupled end-unit (61). Since syringyl units cannot be involved in 5-coupling, dibenzodioxocins have previously been considered to be most prevalent in guaiacyl-rich lignin fractions (58). Finally, the cinnamyl alcohol endgroups **X1**, like the resinols **C**, arise from monomer-monomer coupling and are therefore relatively minor; the deceptively strong **X1** γ-C/H correlation peak is due to the sharpness caused by the relative invariance of proton and carbon chemical shifts in such structures where the bonding is on the aromatic ring, well distant from the γ-position.

The C3H-deficient lignin has a spectrum that has several conspicuous differences. In addition to the relative intensity differences (seen more easily from the volume integral data in Table 3) are two notable structural changes. First, there are no apparent spirodienones **S**, even at contour levels closer to the noise level. Second, there are now several types of dibenzodioxocins **D**, with considerable differences in chemical shifts. The inset in Fig. 3b shows lower contour levels from an experiment run at higher ^{13}C-resolution. Sets of contours labeled **D**1, **D**2 and **D**3 are clearly visible, with only the minor **D**1 pair corresponding to the component observed in the wild-type lignin.

NMR —Long-range Correlations

Long-range correlations (via carbons and protons linked via 2-3 intervening bonds), from HMBC spectra, are valuable in providing information on the types of units (P, G, or S) involved in each linkage type (26, 27, 58, 62). This is because

the carbon chemical shifts in such units are diagnostically different; syringyl 2/6-carbons are at 102-105 ppm; guaiacyl 2-carbons at ~110-112 ppm, guaiacyl 6-carbons at ~ 118-120 ppm, and *p*-hydroxyphenyl 2/6 carbons at 126-130 ppm. Correlations of α-protons in any of the structures to carbons at these disperse frequencies diagnostically determine whether the unit involved is P, G, or S. Although the correlations are not quantitatively relevant, the following are clear from the control lignin spectrum, Fig. 4a: both β-ether **A** and phenylcoumaran **B** units derive from both sinapyl and coniferyl alcohol coupling reactions — they are associated with both syringyl (S) and guaiacyl (G) units; resinol units **C** are essentially all syringyl units, from sinapyl alcohol; arylglycerol units **X7** (as seen only at lower contour levels than shown) are largely syringyl; unfortunately, useful correlations are not evident for dibenzodioxocins **D** using the parameters of this experiment. Interestingly, β-ether units **A** also apparently derive from the low levels of *p*-coumaryl alcohol in the normal plant, suggesting that *p*-coumaryl alcohol efficiently cross-couples with the dominant guaiacyl and/or syringyl units.

HMBC correlations from the C3H-deficient lignin, Fig. 4b, provide the first indications of the coupling and cross-coupling propensities of *p*-coumaryl alcohol and *p*-hydroxyphenyl units (see Discussion Section). The following appear to be evidenced quite clearly: β-ether units **A** are of all three types, P, G and S, but with relatively low levels of the G- (especially) and S-units; the phenylcoumarans **B** are almost entirely P; the dibenzodioxocins **D** now derive from *p*-coumaryl alcohol addition to 5–5-coupled units but, since correlations from G- and S-analogs do not show up in the control, it is not possible to discern whether or not they remain in the C3H-down-regulated material); resinols **C** are no longer just syringyl — syringyl and guaiacyl units are evident, as well as dominant *p*-hydroxyphenyl units for the resinols that have their α-protons displaced to higher chemical shift; arylglycerol units **X7** appear to now derive from all three monolignols, but mainly from sinapyl and *p*-coumaryl alcohols.

DISCUSSION

The NMR spectra reveal both massive and subtle structural differences between the syringyl/guaiacyl lignins in normal wild-type alfalfa vs the *p*-hydroxyphenyl-rich lignins in the heavily C3H-down-regulated plants. They provide the first information regarding the incorporation profile for *p*-coumaryl alcohol into (*p*-hydroxyphenyl-rich) co-polymer lignins. For the first time in such studies, we have attempted to determine whether significant partitioning of lignin structures has occurred during the lignin fractionation and isolation. We analyzed not only the typical solvent-soluble lignins (ML, ~7.6% and 10.8% of the total lignins, Table 1), but also a further sequential fraction from mild acidolysis (51) (AL, another 14.6% and 6.6% of the total lignins) and, more importantly, a major fraction via dissolution of the enzyme lignin (EL) — this latter fraction retains the entire lignin component but our attempts to analyze the whole lignin component, as we have done for various woody samples (52, 63), were thwarted by ending up with only 38% (WT) and 31% (C3H-4a) of this fraction in the $CDCl_3$-soluble NMR fraction (following EDTA washing and molecular weight fractionation). The difficulty in obtaining soluble lignins from alfalfa has been noted previously (36). However, analysis of all three fractions (ML, AL, and EL, Tables 2-3) suggests that neither partitioning of P/G/S

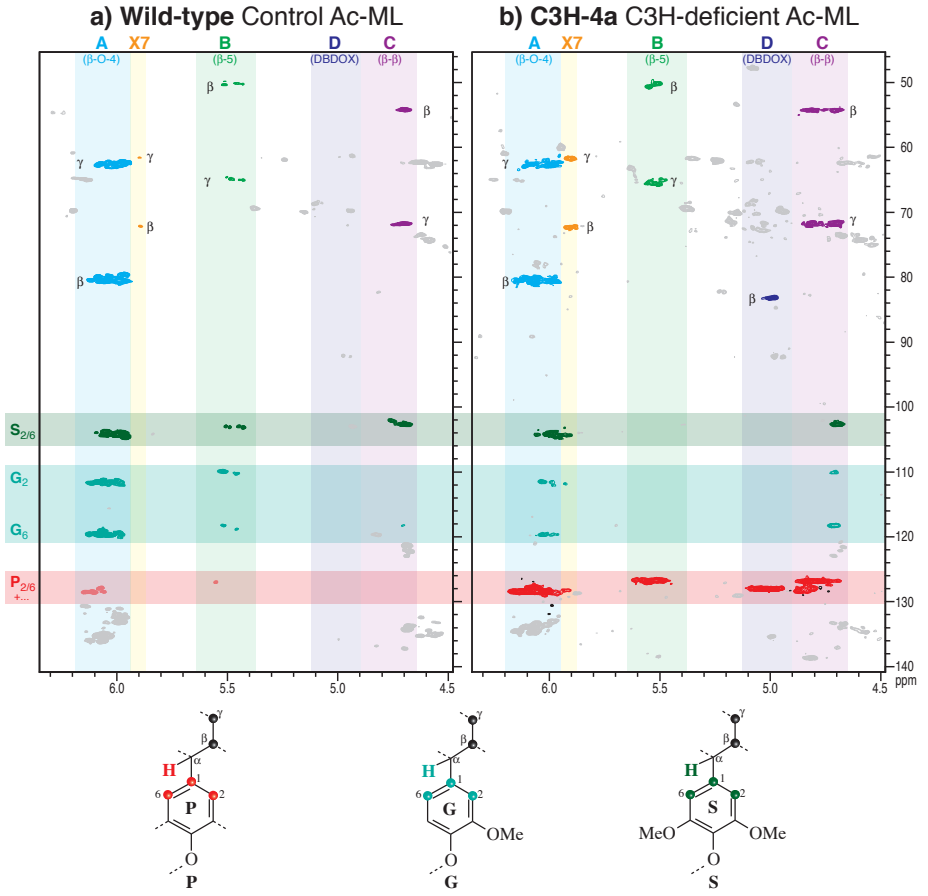

Fig. 4. Partial HMBC spectra of ML lignins isolated from a) the wild-type control and b) the most highly C3H-deficient line, C3H-4a. These long-range (2-3-bond) ^{13}C–^{1}H correlation spectra allow a determination of the monolignol involved in forming each type of structural unit (see Text). The correlations highlighted are from α-protons to the carbons within three bonds, most diagnostically those to the 2- and 6-postions on the aromatic rings of *p*-hydroxyphenyl (P), guaiacyl (G) and syringyl (S) units.

units nor of the various interunit linkage types is a serious issue.

Alfalfa Plants Incorporating High Levels of p-Coumaryl Alcohol

A C3H-deficient Arabidopsis mutant demonstrated that plants without access to the two primary monolignols, coniferyl and sinapyl alcohols (Fig. 1), could be viable, albeit with stunted growth (40). The alfalfa plants here demonstrate that low levels of C3H may result in lignins markedly divergent from those in wild-type controls but with the plants exhibiting more normal growth and development patterns, as is discussed in more detail elsewhere (13). Thus, the C3H-4a line, with about 5% residual C3H-activity and about 55-60% P-lignin content (compared to 1-3% in wild-type), Tables 2-3, grows more slowly and flowers later (Table 1, Fig. 3). However, plants with ~20% residual C3H activity compared to wild-type levels, as in line C3H-9a, restores the growth phenotype to more closely resemble the wild-type (13). Nevertheless, the relative *p*-hydroxyphenyl lignin level is still nearly 10-fold that in the wild-type plant (Table 1). These intermediate level plants will eventually be structurally analyzed in more detail.

Lignin Composition and Structure

The anticipated effect of C3H-deficiency, an enhancement of the relative level of *p*-hydroxyphenyl (P) units in the lignin, is compellingly demonstrated in the aromatic profiles revealed by HSQC NMR spectra, Fig. 2. Wild-type plants have syringyl/guaiacyl lignins with only low levels of P-units. Reduction of C3H depressed the synthesis of coniferyl and sinapyl alcohols although, as noted for all other enzymes in the pathway, not in direct proportion to the enzyme expression level. The most severely down-regulated C3H-4a line (Fig. 2b) was G- and S-depleted and strikingly P-rich, about 65% P (Table 2). At this time, without the availability of a range of model compound data for *p*-hydroxyphenyl-derived dimers and oligomers, only limited assignments of the correlation peaks in this region can be made. The spectra nevertheless demonstrate the dramatically altered composition of the lignins. Further insight, and reasonable quantification of the effects, can be gained by volume-integrating the contours in such spectra. Judiciously choosing only the S2/6, G2, and P2/6 contours assures meaningful comparisons, since these ring-positions are unsubstituted in lignins; carbons-3 and -5 may be carbon- or oxygen-linked and therefore do not show up in these direct ^{13}C–^{1}H correlation spectra. It is necessary to double the G2 contribution to allow for the fact that only a single carbon-proton pair (G2) contributes to this integral in guaiacyl units, vs two pairs (S2/6 or P2/6) in the symmetrical S and P units. The assumption that all S2/6 and G2 units are in the regions indicated is fairly sound, but there is simply not enough model compound data to know whether all P2/6 resonances are in the indicated region. The HSQC-integrals were expected to be quantitatively relevant since they are similar structurally and in an NMR sense. Utilizing dimeric and trimeric model compounds containing mixtures of P, G, and S units showed that essentially no correction is needed and that the "response factors" for each unit type are within a few percent of each other; no corrections are therefore necessary to estimate P:G:S ratios from the volume integrals. As seen in the data of Table 2, the NMR-derived P:G:S ratios are consistent with those ratios derived from degradative methods, Table 1, methods that need not reflect the *actual* ratio of units in the polymer since they measure the distribution only in the relatively low level of monomers that can be released by cleaving β-ether bonds.

The high-field HSQC spectra of the sidechain regions are more revealing regarding the manner in which the monomeric units are assembled. Lignins are characterized by various types of interunit bonds, the most prominent being labeled **A**-**D**, **S**, and **X1** and **X7** in Fig. 3 to retain consistency with standard assignment labeling (1, 3, 58). This linkage-type distribution differs substantially between the wild-type and the C3H-depleted alfalfa lignins. The minor but important spirodienones **S**, resulting from β–1-coupling reactions, are absent in the C3H-deficient lignin. The predominant reaction in lignification is the cross-coupling of a monolignol with the growing polymer. Little enough is known about the cross-coupling of coniferyl and sinapyl alcohols with guaiacyl and syringyl lignins (64), and virtually nothing is known about such reactions involving *p*-coumaryl alcohol. It seems logical from the absence of β–1-coupling products that none of the three monolignols efficiently β–1-couples with P β-ether phenolic end-units in the lignin, nor does *p*-coumaryl alcohol readily β–1-couple with G or S β-ether end-units. As has been discovered with other units, this is likely due to a simple chemical incompatibility. For example, angiosperms efficiently incorporate coniferaldehyde because it will cross-couple with syringyl units (33, 65, 66). However, its *in vitro* or *in vivo* inability to cross-couple with guaiacyl units limits its incorporation into gymnosperm lignins (3).

A multitude of dibenzodioxocins appear in the C3H-deficient lignins. Elucidating the exact nature of these will require considerably more work. The **D**1 correlations match those in a GG/G-dibenzodioxocin model **3b** (Scheme 1) and in the wild-type lignin, so are logically attributable to dibenzodioxocins **D** formed by coupling of a monolignol with 5–5-linked units derived from coupling of two guaiacyl units, i.e. GG/G-, GG/S- or, possibly, GG/P-dibenzodioxocins. The data for the dibenzodioxocin peaks labeled **D**3 (**D**α3 and **D**β3 for the α- and β-C/H correlations) match those for a synthesized PP/P-dibenzodioxocin model **3a** in which all three aromatic nuclei are *p*-hydroxyphenyl (see Materials and Methods). The nature of the large **D**2 correlations remains equivocal. We assumed, from the high levels of P-units in this lignin, it would be an all PP/P-dibenzodioxocin, but the data do not match model **3a**. As noted below from analysis of the HMBC data, it does at least appear to derive from coupling of *p*-coumaryl alcohol to a 5–5-unit. The shifted correlations may be due to 3-substitution on P-units involved in 5–5-coupled structures. Thus PP′/P (where P′ is a 5-linked P-unit) or possibly PG/P dibenzodioxocins seem likely candidates, to be confirmed by future studies.

The other differences in unit-type distribution can be visualized in the spectra but are more readily revealed from data reported in Table 3. Semi-quantification used volume integral correction factors derived from model data, as described in the Materials and Methods Section. The lower proportion of β-ether units **A** (~53-56% vs ~75-80% of the units quantified) is clearly a major reason for the lower thioacidolysis

yields (on a lignin basis) for the C3H-deficient plants vs the wild-type. It also suggests that alkaline pulping efficiency will be lower, since pulping depends on ether cleavage reactions to depolymerize the lignin and render its fragments soluble in the pulping liquor. However, since lignin-polysaccharide cross-linking can occur via trapping of intermediate β-ether quinone methides during lignification, reducing the β-ether content may reduce lignin-polysaccharide cross-linking and produce cell walls that are more enzymatically degradable, as demonstrated for the C3H down-regulated lines via their improved digestibility in ruminant animals (13). Much of the decrease in β-ether **A** levels appears to be due to the two other major units, phenylcoumarans **B** and resinols **C**, each of which nearly doubles in relative proportion. The higher resinol concentration particularly suggests that more monomer-monomer coupling reactions are occurring during the lignification in the P-rich lignins. Although still quite low, the relative dibenzodioxocin **D** level is about double that in wild-type plants. Quantification of cinnamyl alcohol endgroups **X1** was the most variable, but relative levels seem to be similar. Finally, the glycerol structures **X7** are at substantially higher (~8-11-fold) levels. Since it is not known whether glycerol sidechains derive from β-ether units during ball-milling or are produced during lignification, we do not speculate on their relevance at this time. However, we have noted (see Supplementary Material) that oxidative coupling reactions using *p*-coumaryl alcohol produce substantial levels of glycerols (in synthetic polymers that have not been ball-milled) so we are beginning to suspect that they may be, at least in part, authentic units in the native lignins.

Coupling and Cross-coupling Propensities of p-Coumaryl Alcohol in Lignification

Details regarding lignification via enhanced levels of *p*-coumaryl alcohol come from analysis of the HMBC spectra. These spectra allow a determination of which monomers are involved in forming each type of interunit linkage type. The observation from Fig. 4 that essentially all phenylcoumarans **B**, for example, are formed by coupling reactions involving *p*-coumaryl alcohol, is the kind of information that is required to understand the cross-coupling propensity of this monomer. The spectra do not reveal whether the coupling was with a guaiacyl or another *p*-hydroxyphenyl unit, unfortunately. Similarly, the change in resinols **C** from being almost entirely derived from sinapyl alcohol in the wild-type to deriving from all three monomers, and *p*-coumaryl alcohol in particular, in the transgenic plants, is notable. It is logical that sinapyl alcohol monomers find themselves only rarely able to dimerize (with other sinapyl alcohol monomers) in this sinapyl-alcohol-depleted plant, so presumably β–β-cross-couple with coniferyl alcohol, and possibly *p*-coumaryl alcohol; studies are required to determine which of these cross-coupling reactions are chemically feasible, i.e. if sinapyl alcohol and *p*-coumaryl alcohol, for example, are compatible for radical cross-coupling. Examination of thioacidolysis or DFRC dimers by GC-MS (67) may eventually shed light on the occurrence of mixed resinols. Although dibenzodioxocins **D** do not show useful correlations in the wild-type lignins, it appears that the coupling in the C3H-deficient plant also involves coupling of *p*-coumaryl alcohol with the dibenzodioxocin-precursor 5–5-end-unit. The crucial β-aryl ether units derive from all three monolignols, illustrating that *p*-coumaryl alcohol is able to function in the most important endwise-coupling reactions that allow polymer growth. Since *p*-coumaryl alcohol is such a major constituent in these heavily down-regulated plants, the way in which coniferyl and sinapyl alcohols cross-couple with P-units is less clear but should eventually be revealed through studies on alfalfa and other plants with varying levels of down-regulation.

Comments Regarding the Mechanism of Lignification

For decades the accepted theory for lignification is one in which monolignols polymerize largely by radical cross-coupling reactions with the growing polymer in a purely chemical reaction, as recently reviewed (3). A challenge (68) hypothesizes that lignin primary structure could be absolutely dictated by synthesis on arrays of dirigent coupling sites, and replicated by template polymerization. As the review (3) notes, the existing theory explains the current facts and readily explains how massive alterations in the monomer profile may drastically affect lignification and the resulting lignin structure but are readily accommodated by the lignification process. Essentially, since it is simply a chemical process, any phenol finding itself in the cell wall's lignifying zone is capable of entering into the combinatorial free-radical coupling process to the extent allowed by simple chemical concerns such as structural compatibility, and influenced by typical physical parameters such as pH, temperature, ionic strength, and the matrix in general. This is the case here for the at least 20-fold increased levels of the typically minor monolignol, *p*-coumaryl alcohol, but is also seen in more extreme cases. For example, COMT-deficient plants supplant sinapyl alcohol with the non-traditional monomer 5-hydroxyconiferyl alcohol during lignification (33-36). The dirigent array hypothesis encounters difficulty with monomer substitution. The challenge for the new hypothesis remains to explain how a template allows monomer substitution, and to provide direct evidence for ordered macro-structures in lignins. The plant materials examined in the present work may provide materials for such studies.

CONCLUSIONS

Alfalfa lignins strikingly rich in *p*-hydroxyphenyl (P) units are produced by C3H down-regulation. NMR analysis of the lignins suggests that *p*-coumaryl alcohol undergoes coupling and cross-coupling reactions that are for the most part analogous to those of the normally dominant monolignols, coniferyl and sinapyl alcohols. The absence of β–1-structures and a considerable shift in the proportions of others demonstrate that the lignification profile is, however, significantly different. Although the total lignin level appears to be lower in C3H-deficient plants, it is apparent that the plants are substituting the more available *p*-coumaryl alcohol for the normally higher levels of coniferyl and sinapyl alcohols; thus P levels that are typically 1-3% of the lignin rise to ~65% of the lignin in the most heavily down-regulated line. At the extreme, the C3H-deficient Arabidopsis *ref8* mutant (41), which produces lignin at the 100% P level (since it is totally devoid of S and G units), is utilizing the only available monolignol. The compositional and structural changes in the polymer noted

here remain consistent with the existing theory of lignification based on combinatorial radical coupling reactions under simple chemical control.

ACKNOWLEDGEMENTS

The authors thank Dr. Ron Hatfield for carbohydrate analysis. We gratefully acknowledge partial funding through the DOE Energy Biosciences program (#DE-AI02-00ER15067 to JR; DE-FG03-97ER20259 to N.G. Lewis and RAD), and from the Samuel Roberts Noble Foundation and Forage Genetics International (to RAD). NMR experiments on the Bruker DMX-750 cryoprobe system were carried out at the National Magnetic Resonance Facility at Madison with support from the NIH Biomedical Technology Program (RR02301) and additional equipment funding from the University of Wisconsin, NSF Academic Infrastructure Program (BIR-9214394), NIH Shared Instrumentation Program (RR02781, RR08438), NSF Biological Instrumentation Program (DMB-8415048), and the U.S. Department of Agriculture.

Abbreviations

WT: wild type (control)

C3H-4a: most heavily down-regulated transgenic alfalfa line with 5% residual C3H activity

C3H-9a: alfalfa line with 20% residual C3H activity

P: *p*-hydroxyphenyl unit in lignin or *p*-coumaryl alcohol monolignol (depending on context)

G: guaiacyl unit in lignin or coniferyl alcohol monolignol

S: syringyl unit in lignin or sinapyl alcohol monolignol

DHP: dehydrogenation polymer

GG/G-dibenzodioxocin: all guaiacyl dibenzodioxin, c.f. model compound **3b**, Scheme 1

PP/P-dibenzodioxocin: all *p*-hydroxyphenyl dibenzodioxocin, c.f. model compound **3a**, Scheme 1

GC-MS: gas chromatography-mass spectrometry

DFRC: derivatization followed by reductive cleavage (method)

CW: cell wall

ML: Solvent-soluble milled (cell wall) lignin (96:4 dioxane: water soluble fraction)

AL: acidolysis lignin fraction (derived from the ML residue)

EL: enzyme lignin (derived from polysaccharidase treatment of the cell wall)

Ac-ML, Ac-AL, Ac-EL: acetylated fractions.

NMR: nuclear magnetic resonance

HSQC: heteronuclear single quantum correlation

HMBC: heteronuclear multiple-bond correlation

EDTA: ethylenediamine tetraacetic acid

Monolignol Biosynthetic Pathway Enzymes

C3H: *p*-coumarate 3-hydroxylase

CAD: cinnamyl alcohol dehydrogenase

CCR: cinnamoyl-CoA reductase

COMT: caffeic acid *O*-methyl transferase (now known to operate preferentially at the aldehyde level)

CCoAOMT: caffeoyl-CoA *O*-methyltransferase

F5H: ferulate 5-hydroxylase (also referred to as CAld-5H, coniferaldehyde 5-hydroxylase)

HCT: *p*-hydroxycinnamoyl-CoA: quinate shikimate *p*-hydroxycinnamoyltransferase

REFERENCES

1. Boerjan, W., Ralph, J., and Baucher, M. (2003) *Ann. Rev. Plant Biol.* **54**, 519-549
2. Baucher, M., Halpin, C., Petit-Conil, M., and Boerjan, W. (2003) *Crit. Rev. Biochem. Mol. Biol.* **38**(4), 305-350
3. Ralph, J., Lundquist, K., Brunow, G., Lu, F., Kim, H., Schatz, P. F., Marita, J. M., Hatfield, R. D., Ralph, S. A., Christensen, J. H., and Boerjan, W. (2004) *Phytochem. Reviews* **3**(1), 29-60
4. Sederoff, R. R., MacKay, J. J., Ralph, J., and Hatfield, R. D. (1999) *Current Opin. Plant Biol.* **2**(2), 145-152
5. Krause, D. O., Denman, S. E., Mackie, R. I., Morrison, M., Rae, A. L., Attwood, G. T., and McSweeney, C. S. (2003) *Fems Microbiol. Rev.* **27**(5), 663-693
6. Guo, D. G., Chen, F., Wheeler, J., Winder, J., Selman, S., Peterson, M., and Dixon, R. A. (2001) *Transgenic Res.* **10**(5), 457-464
7. He, X., Hall, M. B., Gallo-Meagher, M., and Smith, R. L. (2003) *Crop Sci.* **43**(6), 2240-2251
8. Vailhe, M. A. B., Besle, J. M., Maillot, M. P., Cornu, A., Halpin, C., and Knight, M. (1998) *J. Sci. Food Agric.* **76**(4), 505-514
9. Chen, L., Auh, C.-K., Dowling, P., Bell, J., Chen, F., Hopkins, A., Dixon, R. A., and Wang, Z.-Y. (2003) *Plant Biotechnol. J.* **1**(6), 437-449
10. Barrière, Y., Ralph, J., Méchin, V., Guillaumie, S., Grabber, J. H., Argillier, O., Chabbert, B., and Lapierre, C. (2004) *Comptes Rend. Biologies* **327**(9), 847-860
11. Ralph, J., Guillaume, S., Grabber, J. H., Lapierre, C., and Barrière, Y. (2004) *Comptes Rend. Biologies* **327**(5), 467-479
12. Jung, H.-J. G., Ni, W., Chapple, C. C. S., and Meyer, K. (1999) *J. Sci. Food Agric.* **79**(6), 922-928
13. Reddy, M. S. S., Chen, F., Shadle, G. L., Jackson, L., Aljoe, H., and Dixon, R. A. (2005) *Proc. Nat. Acad. Sci.* **102**(46), 16573-16578
14. Boudet, A. M., and Grima-Pettenati, J. (1996) *Mol. Breed.* **2**(1), 25-39
15. Lapierre, C., Pollet, B., Petit-Conil, M., Toval, G., Romero, J., Pilate, G., Leple, J. C., Boerjan, W., Ferret, V., De Nadai, V., and Jouanin, L. (1999) *Plant Physiol.* **119**(1), 153-163
16. Chen, C. Y., Baucher, M., Christensen, J. H., and Boerjan, W. (2001) *Euphytica* **118**(2), 185-195
17. Baucher, M., Christensen, J. H., Meyermans, H., Chen, C. Y., Van Doorsselaere, J., Leple, J. C., Pilate, G., Petit-Conil, M., Jouanin, L., Chabbert, B., Monties, B., Van Montagu, M., and Boerjan, W. (1998) *Polymer Degradation and Stability* **59**(1-3), 47-52
18. Lapierre, C., Pollet, B., Petit-Conil, M., Pilate, G., Leple, C., Boerjan, W., and Jouanin, L. (2000) *ACS Symposium Series* **742** (Lignin : Historical, Biological, and Materials Perspectives), 145-160
19. Whetten, R., and Sederoff, R. (1991) *Forest Ecology and Management* **43**(3-4), 301-316
20. O'Connell, A., Holt, K., Piquemal, J., Grima-Pettenati, J., Boudet, A., Pollet, B., Lapierre, C., Petit-Conil, M., Schuch, W., and Halpin, C. (2002) *Transgenic Res.* **11**(5), 495-503
21. Chen, C. Y., Baucher, M., Holst Christensen, J., and Boerjan, W. (2001) *Euphytica* **118**(2), 185-195
22. Boerjan, W., Meyermans, H., Chen, C., Baucher, M., Van Doorsselaere, J., Morreel, K., Messens, E., Lapierre, C., Pollet, B., Jouanin, L., Leplé, J. C., Ralph, J., Marita, J. M., Guiney, E., Schuch, W., Petit-Conil, M., and Pilate, G. (2001) in *Molecular Breeding of Woody Plants* (Morohoshi, N., and Komamine, A., eds) pp. Chapter 23: 187-194, Elsevier Science, Amsterdam, The Netherlands
23. Osakabe, K., Tsao, C. C., Li, L., Popko, J. L., Umezawa, T., Carraway, D. T., Smeltzer, R. H., Joshi, C. P., and Chiang, V. L. (1999) *Proc. Natl. Acad. Sci. USA* **96**(16), 8955-8960

24. Humphreys, J. M., Hemm, M. R., and Chapple, C. (1999) *Proc. Natl. Acad. Sci. USA* **96**(18), 10045-10050
25. Meyer, K., Shirley, A. M., Cusumano, J. C., Bell-Lelong, D. A., and Chapple, C. (1998) *Proc. Natl. Acad. Sci. USA* **95**(12), 6619-6623
26. Marita, J., Ralph, J., Hatfield, R. D., and Chapple, C. (1999) *Proc. Natl. Acad. Sci. USA* **96**(22), 12328-12332
27. Li, L., Zhou, Y., Cheng, X., Sun, J., Marita, J. M., Ralph, J., and Chiang, V. L. (2003) *Proc. Nat. Acad. Sci.* **100**(8), 4939-4944
28. Huntley, S. K., Ellis, D., Gilbert, M., Chapple, C., and Mansfield, S. D. (2003) *J. Agric. Food Chem.* **51**(21), 6178-6183
29. Baucher, M., Monties, B., Van Montagu, M., and Boerjan, W. (1998) *Crit. Rev. in Plant Sci.* **17**(2), 125-197
30. Ralph, J. (1996) *J. Nat. Prod.* **59**(4), 341-342
31. Morrison, W. H., Akin, D. E., Archibald, D. D., Dodd, R. B., and Raymer, P. L. (1999) *Industrial Crops and Products* **10**(1), 21-34
32. Li, L., Popko, J. L., Umezawa, T., and Chiang, V. L. (2000) *J. Biol. Chem.* **275**(9), 6537-6545
33. Ralph, J., Lapierre, C., Marita, J., Kim, H., Lu, F., Hatfield, R. D., Ralph, S. A., Chapple, C., Franke, R., Hemm, M. R., Van Doorsselaere, J., Sederoff, R. R., O'Malley, D. M., Scott, J. T., MacKay, J. J., Yahiaoui, N., Boudet, A.-M., Pean, M., Pilate, G., Jouanin, L., and Boerjan, W. (2001) *Phytochem.* **57**(6), 993-1003
34. Ralph, J., Lapierre, C., Lu, F., Marita, J. M., Pilate, G., Van Doorsselaere, J., Boerjan, W., and Jouanin, L. (2001) *J. Agric. Food Chem.* **49**(1), 86-91
35. Marita, J. M., Ralph, J., Lapierre, C., Jouanin, L., and Boerjan, W. (2001) *J. Chem. Soc., Perkin Trans. 1* (22), 2939-2945
36. Marita, J. M., Ralph, J., Hatfield, R. D., Guo, D., Chen, F., and Dixon, R. A. (2003) *Phytochem.* **62**(1), 53-65
37. Sarkanen, K. V., and Hergert, H. L. (1971) in *Lignins. Occurrence, Formation, Structure and Reactions* (Sarkanen, K. V., and Ludwig, C. H., eds) pp. 43-94, Wiley-Interscience, New York
38. Ralph, J., Hatfield, R. D., Quideau, S., Helm, R. F., Grabber, J. H., and Jung, H.-J. G. (1994) *J. Amer. Chem. Soc.* **116**(21), 9448-9456
39. Timmel, T. E. (1986) *Compression wood in gymnosperms*, Springer, Heidelberg
40. Franke, R., Humphreys, J. M., Hemm, M. R., Denault, J. W., Ruegger, M. O., Cusumano, J. C., and Chapple, C. (2002) *Plant J.* **30**(1), 33-45
41. Franke, R., Hemm, M. R., Denault, J. W., Ruegger, M. O., Humphreys, J. M., and Chapple, C. (2002) *Plant J.* **30**(1), 47-59
42. Schoch, G., Goepfert, S., Morant, M., Hehn, A., Meyer, D., Ullmann, P., and Werck-Reichhart, D. (2001) *J. Biol. Chem.* **276**(39), 36566-36574
43. Fukushima, R. S., and Hatfield, R. D. (2001) *J. Agric. Food Chem.* **49**(7), 3133-3139
44. Rolando, C., Monties, B., and Lapierre, C. (1992) in *Methods in Lignin Chemistry* (Dence, C. W., and Lin, S. Y., eds) pp. 334-349, Springer-Verlag, Berlin-Heidelberg
45. Lu, F., and Ralph, J. (1997) *J. Agric. Food Chem.* **45**(12), 4655-4660
46. Lu, F., and Ralph, J. (1999) *J. Agric. Food Chem.* **47**(5), 1988-1992
47. Hatfield, R. D., and Weimer, P. J. (1995) *J. Sci. Food Agric.* **69**(2), 185-196
48. Ralph, S. A., Landucci, L. L., and Ralph, J. (2005) NMR Database of Lignin and Cell Wall Model Compounds. In. *Available over Internet at http://ars.usda.gov/Services/docs.htm?docid=10429 (previously http://www.dfrc.ars.usda.gov/software.html), updated at least annually since 1993*
49. Morreel, K., Ralph, J., Kim, H., Lu, F., Goeminne, G., Ralph, S. A., Messens, E., and Boerjan, W. (2004) *Plant Physiol.* **136**(3), 3537-3549
50. Ralph, J., Hatfield, R. D., Piquemal, J., Yahiaoui, N., Pean, M., Lapierre, C., and Boudet, A.-M. (1998) *Proc. Nat. Acad. Sci.* **95**(22), 12803-12808
51. Wu, S., and Argyropoulos, D. S. (2003) *J. Pulp Paper Sci.* **29**(7), 235-240
52. Lu, F., and Ralph, J. (2003) *Plant J.* **35**(4), 535-544
53. Quideau, S., and Ralph, J. (1994) *Holzforschung* **48**(1), 12-22
54. Reinhoudt, D. N., Dejong, F., and Vandevondervoort, E. M. (1981) *Tetrahedron* **37**(9), 1753-1762
55. Quideau, S., and Ralph, J. (1992) *J. Agric. Food Chem.* **40**(7), 1108-1110
56. Landucci, L. L., Luque, S., and Ralph, S. A. (1995) *J. Wood Chem. Tech.* **15**(4), 493-513
57. Nakano, J., and Meshitsuka, G. (1992) in *Methods in Lignin Chemistry* (Lin, S. Y., and Dence, C. W., eds) pp. 23-32, Springer-Verlag, Heidelberg
58. Ralph, J., Marita, J. M., Ralph, S. A., Hatfield, R. D., Lu, F., Ede, R. M., Peng, J., Quideau, S., Helm, R. F., Grabber, J. H., Kim, H., Jimenez-Monteon, G., Zhang, Y., Jung, H.-J. G., Landucci, L. L., MacKay, J. J., Sederoff, R. R., Chapple, C., and Boudet, A. M. (1999) in *Advances in Lignocellulosics Characterization* (Argyropoulos, D. S., and Rials, T., eds) pp. 55-108, TAPPI Press, Atlanta, GA
59. Zhang, L., and Gellerstedt, G. (2001) *Chem. Commun.* (24), 2744-2745
60. Zhang, L., Gellerstedt, G., Lu, F., and Ralph, J. (2006) *J. Wood Chem. Technol.*, in press
61. Karhunen, P., Rummakko, P., Sipilä, J., Brunow, G., and Kilpeläinen, I. (1995) *Tetrahedron Lett.* **36**(1), 169-170
62. Hu, W.-J., Lung, J., Harding, S. A., Popko, J. L., Ralph, J., Stokke, D. D., Tsai, C.-J., and Chiang, V. L. (1999) *Nature Biotechnol.* **17**(8), 808-812
63. Ralph, J., and Lu, F. (2004) *Org. Biomol. Chem.* **2**(19), 2714-2715
64. Syrjanen, K., and Brunow, G. (2000) *J. Chem. Soc. Perkin Trans. 1* (2), 183-187
65. Kim, H., Ralph, J., Yahiaoui, N., Pean, M., and Boudet, A.-M. (2000) *Org. Lett.* **2**(15), 2197-2200
66. Kim, H., Ralph, J., Lu, F., Ralph, S. A., Boudet, A.-M., MacKay, J. J., Sederoff, R. R., Ito, T., Kawai, S., Ohashi, H., and Higuchi, T. (2003) *Org. Biomol. Chem.* **1**, 158-281
67. Lapierre, C. (1993) in *Forage Cell Wall Structure and Digestibility* (Jung, H. G., Buxton, D. R., Hatfield, R. D., and Ralph, J., eds) pp. 133-166, ASA-CSSA-SSSA, Madison, WI
68. Gang, D. R., Costa, M. A., Fujita, M., Dinkova-Kostova, A. T., Wang, H. B., Burlat, V., Martin, W., Sarkanen, S., Davin, L. B., and Lewis, N. G. (1999) *Chem. Biol.* **6**(3), 143-151
69. Grabber, J. H., Hatfield, R. D., and Ralph, J. (2003) *J. Agric. Food Chem.* **51**(17), 4984-4989
70. Kim, H., and Ralph, J. (2005) *J. Agric. Food Chem.* **53**(9), 3693-3695
71. Landucci, L. L. (2000) *J. Wood Chem. Technol.* **20**(3), 243-264

Effects of Coumarate 3-Hydroxylase Down-regulation on Lignin Structure

John Ralph,*[,1,2] Takuya Akiyama,[1] Hoon Kim,[1,3] Fachuang Lu,[1,2] Paul F. Schatz,[1] Jane M. Marita,[1] and Sally A. Ralph.[4]

From the [1]U.S. Dairy Forage Research Center, USDA-Agricultural Research Service, Madison Wisconsin 53706, USA; [2]Department of Forestry, and [3]Department of Horticulture, University of Wisconsin, Madison, Wisconsin 53706, USA; [4]U.S. Forest Products Laboratory, USDA-Forest Service, Madison, Wisconsin 53705, USA.

M. S. Srinivasa Reddy,[5] Fang Chen,[5] and Richard A. Dixon.[5]

From the [5]Plant Biology Division, Samuel Roberts Noble Foundation, Ardmore, Oklahoma 73401, USA.

SUPPLEMENTARY MATERIAL

This supplementary data is largely to document the NMR analysis of other lignin fractions and synthetic lignin models that are mentioned in the main paper but are not crucial to it.

The figure numbers conform with those in the manuscript. The original figures (without photographic insets) from the paper are included here on the same scale.

SUPPLEMENTARY MATERIALS AND METHODS

Synthetic Lignins (DHPs)

Synthetic dehydrogenation polymers (DHPs) are useful to illustrate the attribution of assignment data, e.g. to P vs G vs S in the aromatic regions of HSQC spectra, Fig. 2. They were prepared by slow independent addition of monomers and H_2O_2 via a peristaltic pump (69) to peroxidase enzyme (Sigma #P8250, Type II, 150-250 units/mg solid, Sigma-Aldrich, Milwaukee, WI) in pH 6.8 phosphate buffer. *p*-Coumaryl alcohol was synthesized by DIBAL-H reduction of ethyl *p*-coumarate which was prepared from *p*-coumaric acid (55). Coniferyl and sinapyl alcohols were prepared from the corresponding 4-hydroxycinnamyl aldehydes (70).

p-Coumaryl alcohol DHP (P-DHP). *p*-Coumaryl alcohol (200 mg) was dissolved in dioxane (30 ml) and distilled water (70 ml) was added (flask #1). 30% H_2O_2 (181 µl; 1.2 eq.) was mixed with 100 ml of distilled water (flask #2) giving a slightly cloudy solution. Horseradish peroxidase (5.52 mg; 181 units/mg) was prepared in 40 ml of 50 mM sodium phosphate buffer (pH 6.8, flask #3). Flask #1 and #2 were connected to independent viton lines which were pumped over 25 h. into the flask #3 through using a multi-channel peristaltic pump at a rate of 4 ml/h. Flasks were covered with aluminum foil to limit light during the reaction. Horseradish peroxidase (8.29 mg) was added once more, and the reaction was stirred for and additional 24 hours at room temperature. The precipitate were simply filtered through a fine-porosity sintered glass Buchner filter. A light-brown colored crude product (200 mg) was obtained. Acetylation of the P-DHP (120 mg) in acetic anhydride/pyridine was at 50 °C for 24 hours (the DHP would not dissolve in the reaction medium at room temperature). The resultant acetylated P-DHP (178 mg) was not fully soluble in acetone or chloroform. After sonicating in chloroform, the dark solution was filtered and dried under reduced pressure yielding just 66 mg of soluble acetylated P-DHP.

Mixed PGS-DHP. The three monolignols (*p*-Coumaryl alcohol P: 200 mg, 0.7 eq.; coniferyl alcohol G: 51.4 mg, 0.15 eq.; sinapyl alcohol S: 60 mg, 0.15 eq.) were dissolved in dioxane (45 ml) and distilled water (105 ml) was added giving a slightly cloudy solution (flask #1). 30% H_2O_2 (284 µl; 1.2 eq.) was mixed with 150 ml of distilled water (flask #2). Horseradish peroxidase (8.29 mg x 2; 181 units/mg) was prepared in 60 ml of 50 mM sodium phosphate buffer (pH 6.8) (flask #3). Flask #1 and #2 were connected to independent viton lines which were pumped into the flask #3 through using a multi-channel peristaltic pump at a rate of 3 ml/h. Flasks were covered with aluminum foil to limit light during the reaction. The reaction was stirred for 50 hours at room temperature. Horseradish peroxidase (8.29 mg) was added once more after 25 hours. The precipitate was simply filtered out through a fine-porosity sintered glass Buchner filter. A brown colored crude product (325 mg) was obtained. Acetylation of the PGS-DHP (225 mg) in acetic anhydride/pyridine was at 50 °C for 24 hours. Acetylated PGS-DHP (325 mg) was not fully soluble in acetone or chloroform. After sonicating in chloroform, the insoluble black solid was filtered off and the soluble fraction dried under reduced pressure yielding just 30 mg of soluble acetylated PGS-DHP. No attempts were made to characterize the remaining fractions.

SUPPLEMENTARY MATERIAL

FIGURE CAPTIONS

Figures 2. Partial short-range $^{13}C–^{1}H$ (HSQC) correlation spectra (aromatic regions only) of milled lignins (ML) isolated from a) the wild-type control and b) the most highly C3H-deficient line, C3H-4a. (Augment Fig. 2 in the paper, showing how the three lignin isolates are similar). Traces of *p*-hydroxyphenyl (P) units are seen in the typically syringyl/guaiacyl lignin in the wild-type alfalfa, whereas P-units entirely dominate the spectrum in the transgenic. The spectra from the various lignin isolates are almost identical (although plotting at the same contour levels was not possible). Semi-quantitative volume integrals are given in Table 2. **2A**) Solvent-soluble lignins, ML (as in Fig. 2 in the paper). **2B**) Acidolysis lignins, AL. **2C**) Polysaccharidase-digested cell walls following CW dissolution, $CHCl_3$-fractionation, and EDTA washing (as noted in the Materials and Methods Section), "Enzyme Lignin" EL. **2D**) Synthetic lignins made from a) coniferyl + sinapyl alcohols using the $Mn(OAc)_3$ in pyridine via the described previously (71) — this lignin has considerable benzylic oxidation resulting in the syringyl (green) peaks displaced to (7.0-7.35)/(106-107) ppm, and b) from *p*-coumaryl alcohol via peroxidase as described in the Supplementary Experimental Section.

Figures 3. Partial short-range $^{13}C–^{1}H$ (HSQC) spectra (sidechain regions) of milled lignins (ML) isolated from a) the wild-type control and b) the most highly C3H-deficient line, C3H-4a. (Augment Fig. 3 in the paper). C3H-deficiency, and the incorporation of higher levels of *p*-coumaryl alcohol into the lignin, produces significant changes in the distribution of interunit linkage types. Interunit type designations **A**-**D**, **S** (**F**), **X1** and **X7** follow conventions established previously (1, 3, 58). Attempts to designate polysaccharide-derived contours in grey rather than black were not always possible due to spectral congestion. Volume integrals and semi-quantitative data are given in Table 3. **3A**) Solvent-soluble lignins, ML (as in Fig. 2 in the paper). The absence of spirodienone S units in the transgenic reveals that *p*-coumaryl alcohol does not apparently favor β–1-cross-coupling reactions. Several types of new dibenzodioxocins **D** are more readily seen at the lower contour levels in the more highly resolved partial spectrum in the inset. Note that the contour levels used to display the two spectra were chosen to highlight the structural similarities and differences; with no internally invariant peaks, interpretation of apparent visual quantitative differences needs to be cautious. **3B**) Acidolysis lignins, AL; note that spirodienones **S** are converted to open β–1-structures **F** on acidolysis. **3C**) Polysaccharidase-digested cell walls following CW dissolution, $CHCl_3$-fractionation, and EDTA washing (as noted in the Materials and Methods Section), "Enzyme Lignin" EL; obviously these fractions contain a much higher polysaccharide component, but most of the lignin correlations remain well-resolved. **3D**) Synthetic lignins made from a) coniferyl + sinapyl alcohols as described above, which has a very high β-ether **A** content and essentially no phenylcoumarans **B**, and b) from *p*-coumaryl alcohol via peroxidase as described in the Supplementary Experimental Section below. Note that both of these spectra contain substantial arylglycerol **X7** contours despite having not been ball-milled; apparently glycerols can be formed under both metal- and peroxidase-assisted coupling conditions.

Fig. 2A. Solvent-soluble Lignins, ML (c.f. Fig. 2 in the paper)

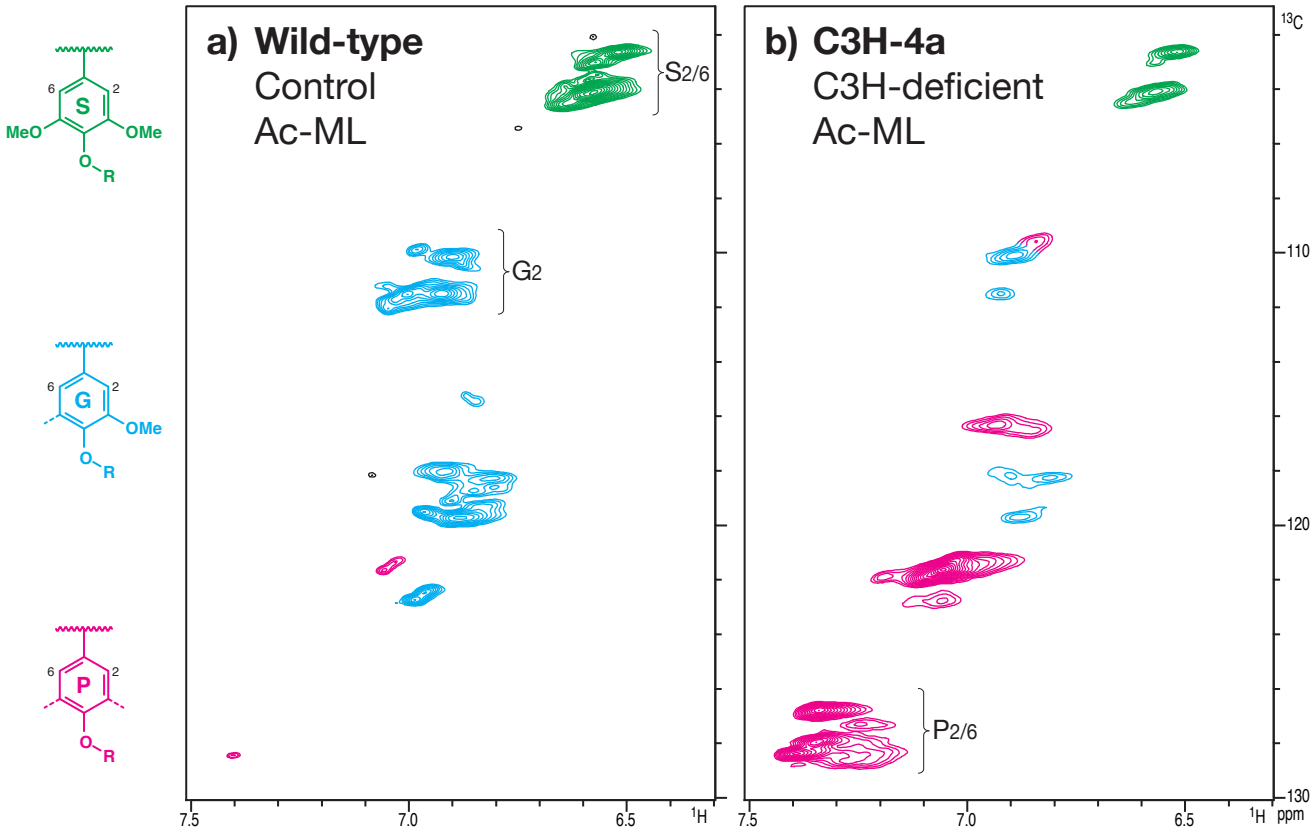

Fig. 2B. Acidolysis Lignins, AL (see Fig. 2 in the paper for ML)

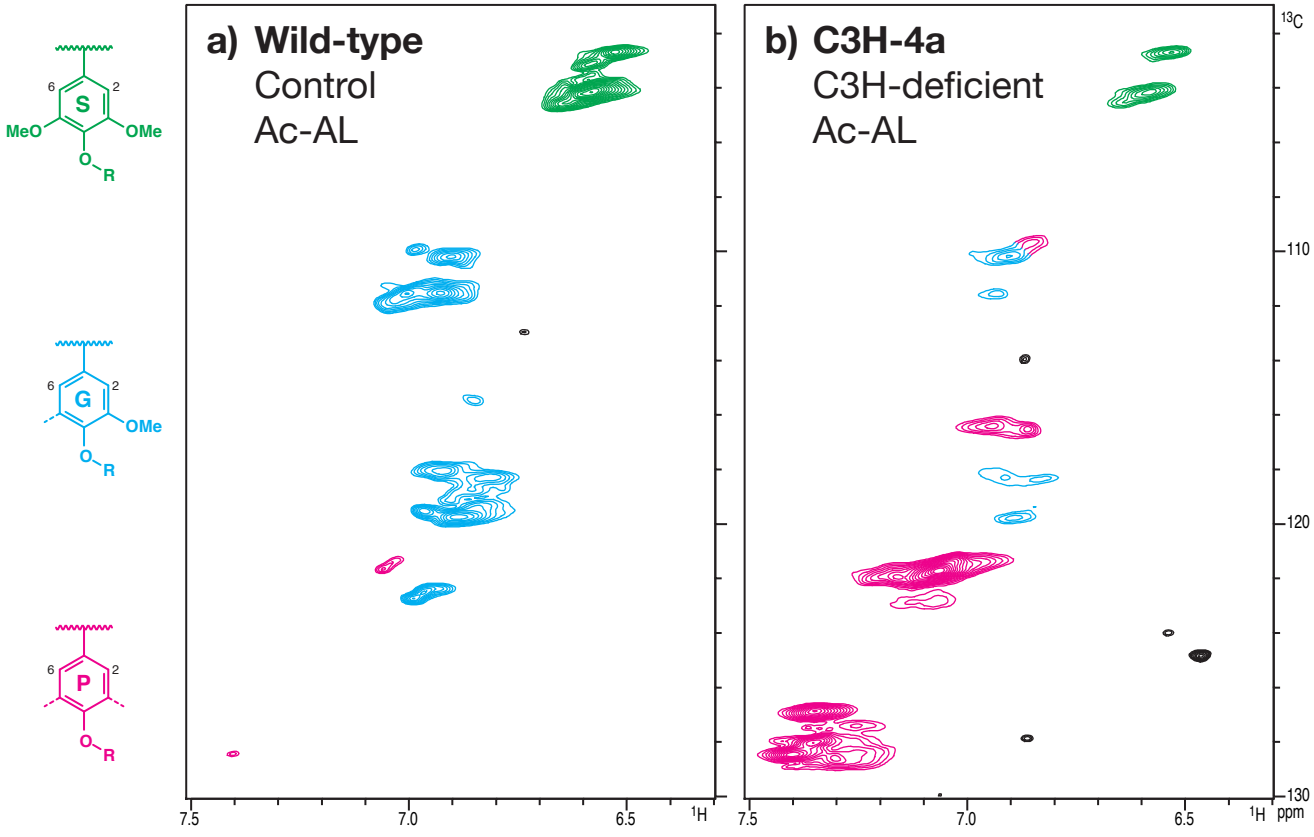

Fig. 2C. Enzyme Lignins, EL (see Fig. 2 in the paper for ML)

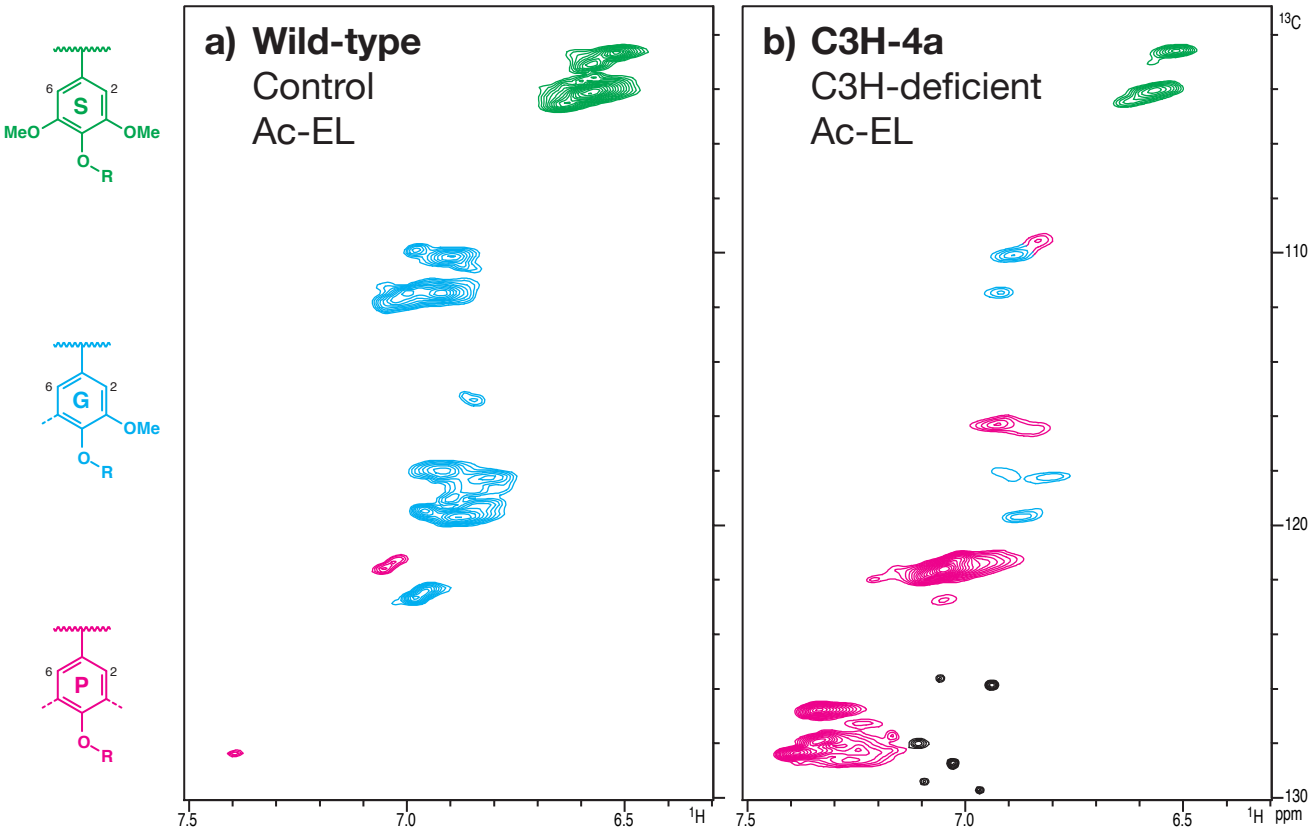

Fig. 2D. Synthetic Lignins (DHPs) (see Fig. 2 in the paper for ML)

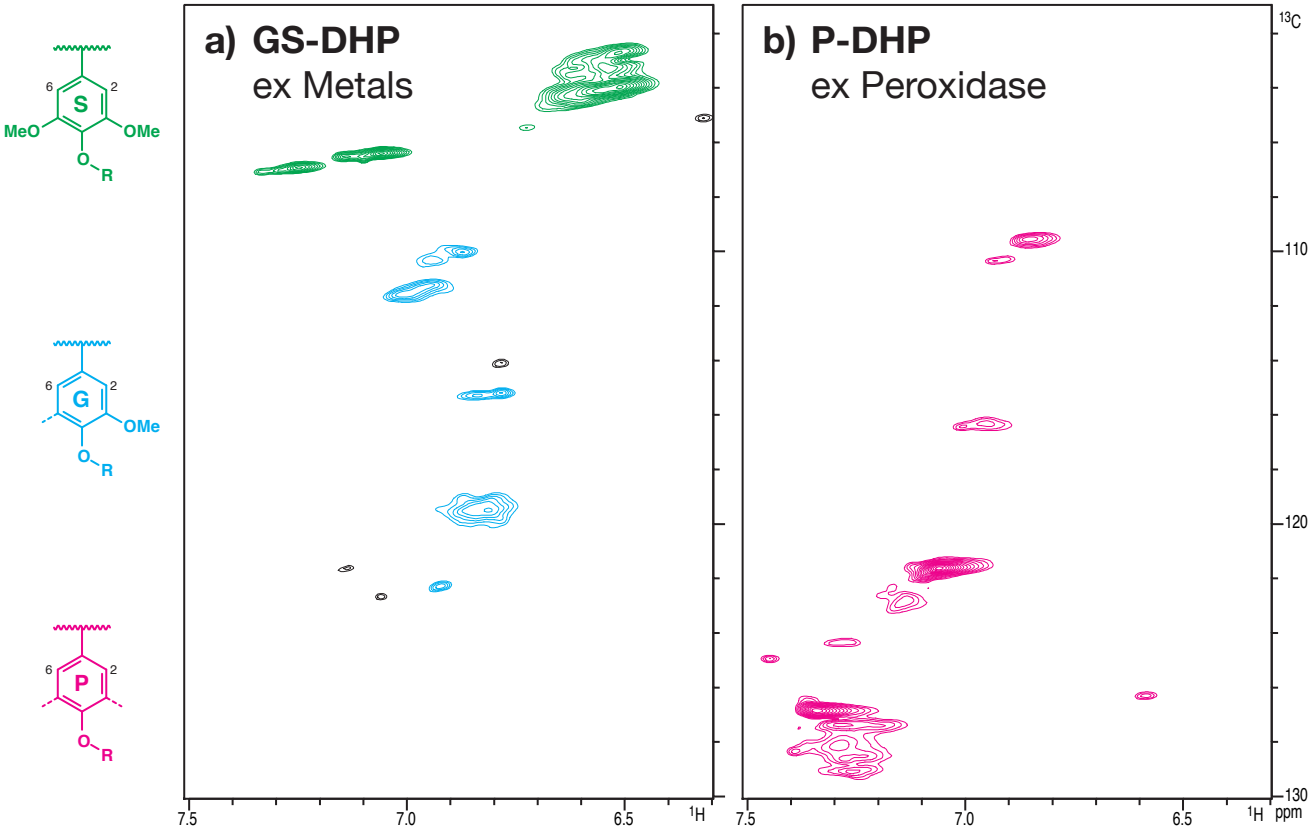

Fig. 3A.
Solvent-soluble Lignins
(c.f. Fig. 3 in the paper)

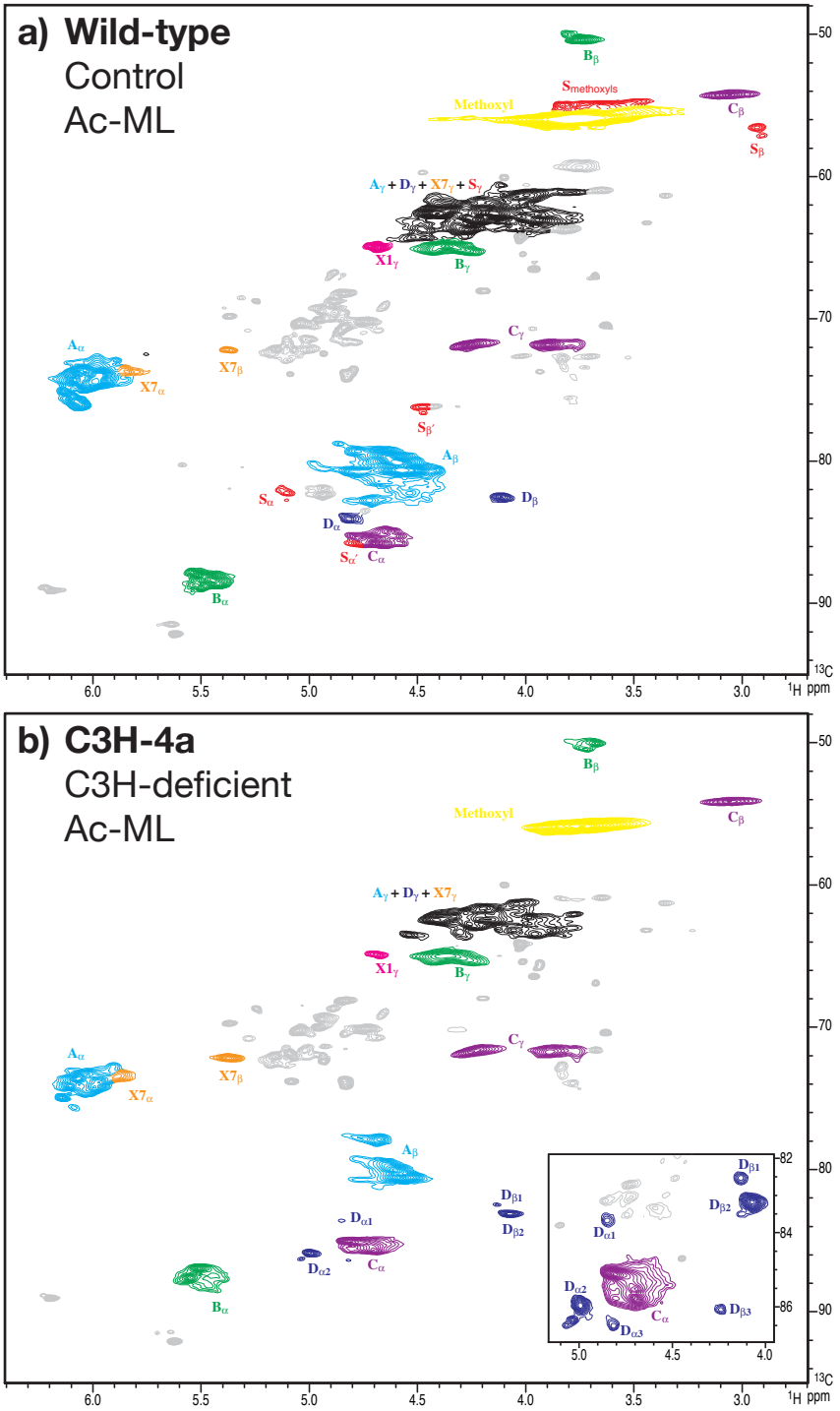

Fig. 3B. Acidolysis Lignins, AL (see Fig. 2 in the paper for ML)

(note that spirodienones **S** get converted to β–1-structures **F** on acidolysis!)

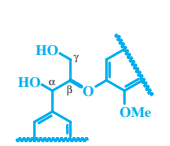

A
β-aryl ether
(β-O-4)

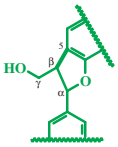

B
phenylcoumaran
β-5 (α-O-4)

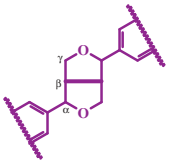

C
resinol
β-β (α-O-γ)

D
dibenzodioxocin
5-5/β-O-4 (α-O-4)

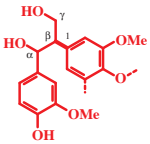

F
β-1 (open)

Methoxyl

Unresolved

Unassigned,
saccharides etc.

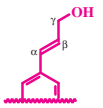

X1
cinnamyl
alcohol

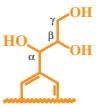

X7
arylglycerol

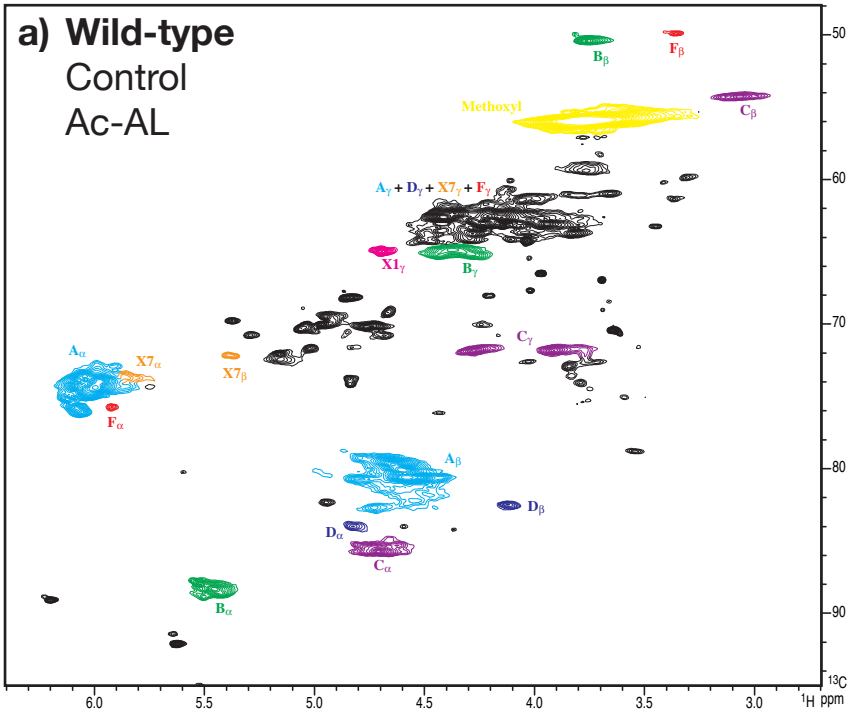

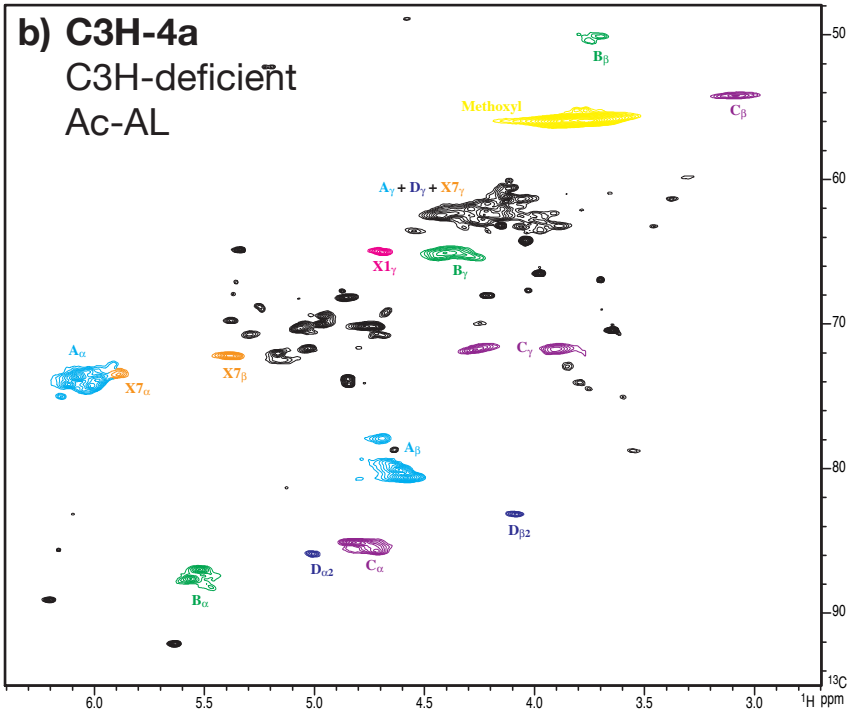

Fig. 3C. Enzyme Lignins, EL (see Fig. 2 in the paper for ML)

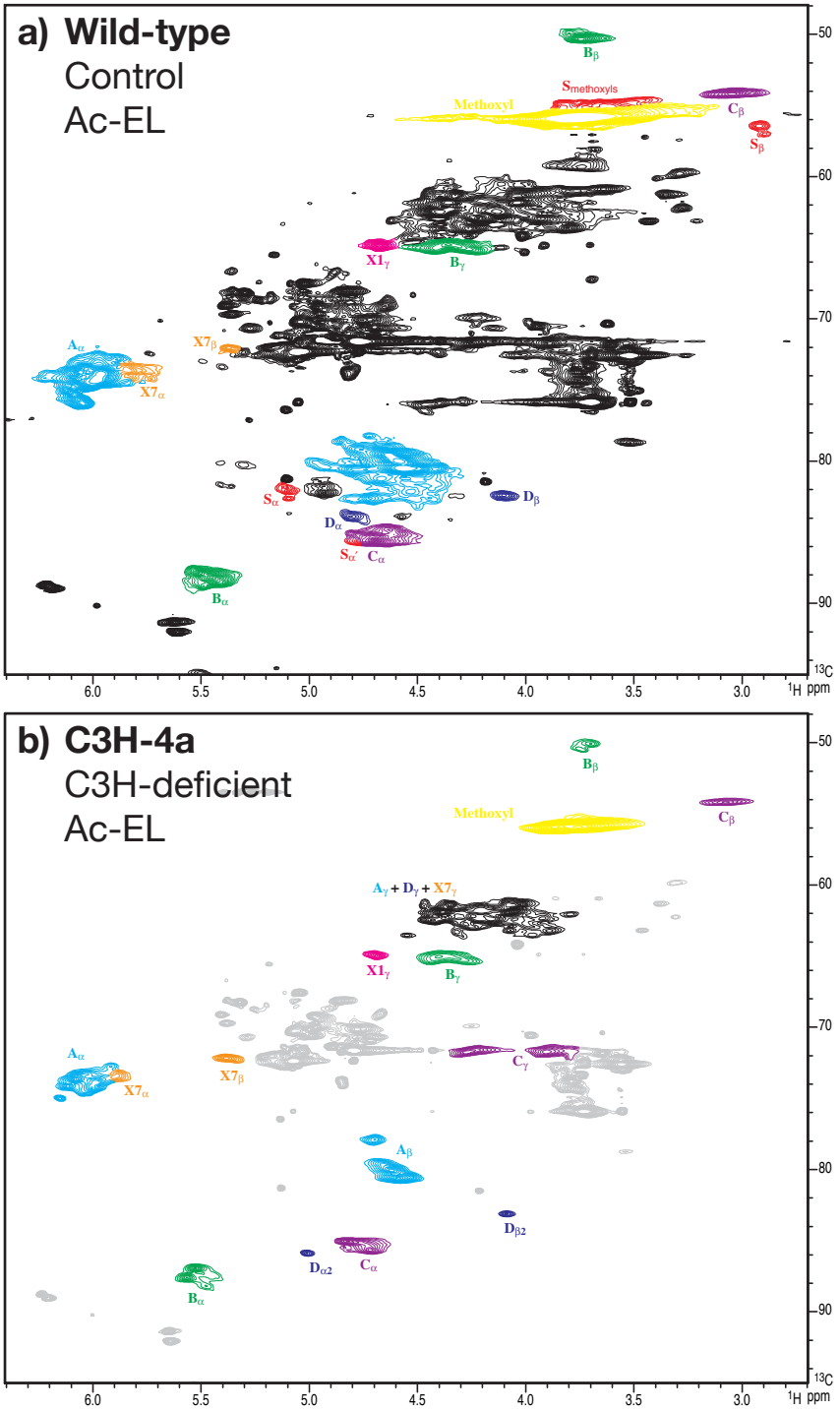

A
β-aryl ether
(β-O-4)

B
phenylcoumaran
β-5 (α-O-4)

C
resinol
β-β (α-O-γ)

D
dibenzodioxocin
5-5/β-O-4 (α-O-4)

S
spirodienone
β-1 (α-O-α)

Methoxyl

Unresolved

Unassigned,
saccharides etc.

X1
cinnamyl
alcohol

X7
arylglycerol

Fig. 3D. Synthetic Lignins (DHPs) (see Fig. 2 in the paper for ML)

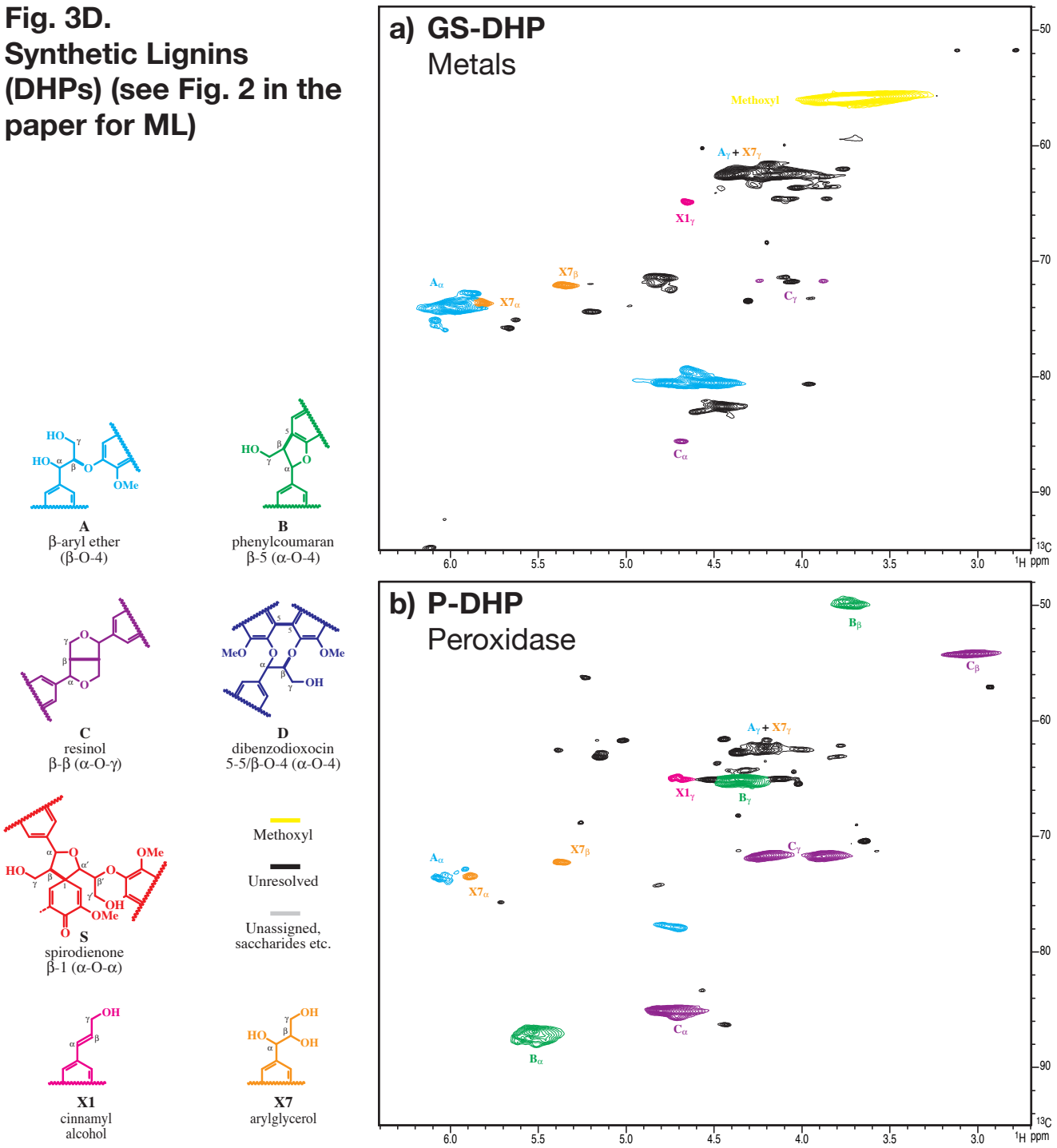

A
β-aryl ether
(β-O-4)

B
phenylcoumaran
β-5 (α-O-4)

C
resinol
β-β (α-O-γ)

D
dibenzodioxocin
5-5/β-O-4 (α-O-4)

S
spirodienone
β-1 (α-O-α)

Methoxyl

Unresolved

Unassigned,
saccharides etc.

X1
cinnamyl
alcohol

X7
arylglycerol